HOT EXTRUSION OF ALPHA PHASE URANIUM-ZIRCONIUM ALLOYS FOR TRU BURNING FAST REACTORS

A Thesis

by

JEFFREY STEPHEN HAUSAMAN

Submitted to the Office of Graduate Studies of
Texas A&M University
in partial fulfillment of the requirements for the degree of

MASTER OF SCIENCE

December 2011

Major Subject: Nuclear Engineering

Hot Extrusion of Alpha Phase Uranium-Zirconium Alloys for TRU Burning Fast Reactors

HOT EXTRUSION OF ALPHA PHASE URNIUM-ZIRCONIUM ALLOYS

FOR TRU BURNING FAST REACTORS

A Thesis

by

JEFFREY STEPHEN HAUSAMAN

Submitted to the Office of Graduate Studies of
Texas A&M University
in partial fulfillment of the requirements for the degree of

MASTER OF SCIENCE

Approved by:

Chair of Committee,	Sean M. McDeavitt
Committee Members,	William S. Charlton
	Jaime C. Grunlan
	Lin Shao
Head of Department,	Raymond J. Juzaitis

December 2011

Major Subject: Nuclear Engineering

ABSTRACT

Hot Extrusion of Alpha Phase Uranium-Zirconium Alloys for TRU Burning Fast Reactors. (December 2011)

Jeffrey Stephen Hausaman, B.S., Texas A&M University

Chair of Advisory Committee: Dr. Sean M. McDeavitt

The development of fast reactor systems capable of burning recycled transuranic (TRU) isotopes has been underway for decades at various levels of activity. These systems could significantly alleviate nuclear waste storage liabilities by consuming the long-lived isotopes of plutonium (Pu), neptunium (Np), americium (Am), and curium (Cm). The fabrication of metal fuel alloys by melt casting pins containing the volatile elements Am and Np has been a major challenge due to their low vapor pressures; initial trials demonstrated significant losses during the casting process.

A low temperature hot extrusion process was explored as a potential method to fabricate uranium-zirconium fuel alloys containing the TRU isotopes. The advantage of extrusion is that metal powders may be mixed and enclosed in process canisters to produce the desired composition and contain volatile components. Uranium powder was produced for the extrusion process by utilizing a hydride-dehydride process that was developed in conjunction with uranium alloy sintering studies. The extrusions occurred at 600ºC and utilized a hydraulic press capable of 450,000 N (50 tons) of force.

Magnesium (Mg) metal was used as a surrogate metal for Pu and Am because of its low melting point (648°C) and relatively high vapor pressure (0.2 atm at 725°C). Samples containing U, Zr, and Mg powder were prepared in an inert atmosphere glovebox using copper canisters and extruded at 600°C. The successful products of the extrusion method were characterized using thermal analysis with a differential scanning calorimeter as well as image and x-ray analysis utilizing an electron microprobe. The analysis showed that upon fabrication the matrix of the extruded metal alloy is completely heterogeneous with no mixing of the metal particle constituents. Further heat treating upon this alloy allows these different materials to interdiffuse and form mixed uranium-zirconium phases with varying types of microstructures. Image and x-ray analysis showed that the magnesium surrogate present in a sample was retained with little evidence of losses due to vaporization.

DEDICATION

I'd like to dedicate this thesis to my family and friends, for always believing in my ability and encouraging me to succeed in my graduate studies.

ACKNOWLEDGEMENTS

I would like to acknowledge the wisdom and guidance of Dr. McDeavitt, my committee chair, throughout my undergraduate and graduate studies. Also, I would like to acknowledge the rest of my committee; Dr. Charlton, Dr. Grunlan and Dr. Shao for their contributions to this thesis, as well as their collective roles in my undergraduate and graduate education.

I would like to acknowledge the members of staff of the Fuel Cycle and Materials Laboratory for their invaluable assistance in helping me complete this work. This includes, but is not limited to (in no particular order): Aaron Totemier, Adam Parkison, David Garnetti, Grant Helmreich, Carissa Humrickhouse, Micheal Naramore, Jeffrey Clemens, Brandon Blamer, Daniel Eichel, Julie Borgmeyer, and Allison Cosgrove. I would also like to acknowledge the support and exceptional learning environment provided by the entire Texas A&M University Department of Nuclear Engineering.

I would also like to acknowledge Dr. Guillemette of the Department of Geology for exceptional assistance in teaching and training me to utilize the electron microprobe, which was an indispensable component to this research.

I would also like to acknowledge Braden Goddard and Alice Dale for being exceptional friends and colleagues.

TABLE OF CONTENTS

Page

LIST OF FIGURES

LIST OF TABLES

1. INTRODUCTION

Nuclear reactors systems generate fission products and activation products within the fuel. The activation products include the transuranic (TRU) isotopes of neptunium (Np), plutonium (Pu), americium (Am), and curium (Cm). Fast reactor systems, so named because of their primary reliance on high energy ("fast") neutrons, have the ability to consume the TRU isotopes to generate energy, but this requires processing. If TRU recycling methods and fast reactors are employed, a full-scale fuel fabrication method must be developed to generate fuel to supply a full core of TRU-bearing fuel rods.

1.1 METAL FUEL FABRICATION ISSUES

The method of fabricating metal fuel elements for fast reactor systems has historically been an injection casting method, which was utilized for reactors such as Experimental Breeder Reactor II[1]. Molten uranium alloy mix in a crucible at approximately 1500°C is drawn up into quartz mold driven by a pressure differential between the molten pool and the interior of the mold. After injection, the molds are allowed to cool and broken open to produce a cast fuel pin, which is then machined to the required specifications[2]. This method has some known issues, specifically the material exchange between the quartz mold and the cast alloy. This results in a ring of silicon on the outside of the fuel pin as well as the quartz molds acquiring radioactive constituents of the fuel which necessitates their treatment as high level waste[3].

This thesis follows the style of Journal of Nuclear Materials.

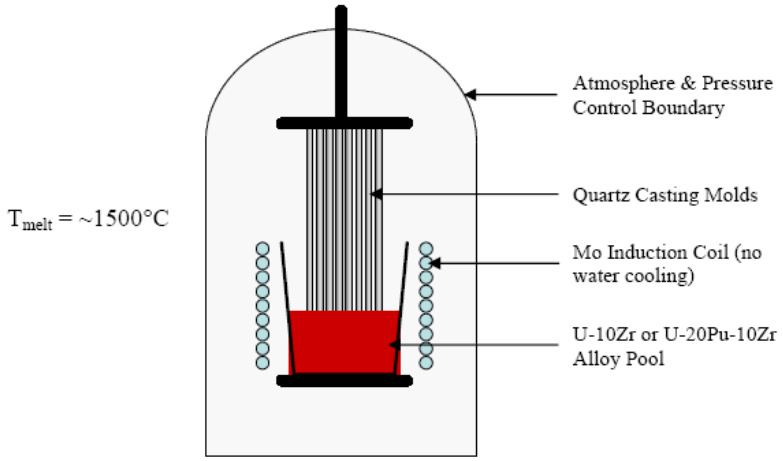

Figure (1-1) Simplified Diagram of injection casting process[4]

In addition to material losses and alloy contamination due to the injection casting process, diagrammed in FIGURE (1-1), introducing the transuranic elements americium (Am) and curium (Cm) into the casting caused evaporative losses due to the high vapor pressure they possess at the temperature that uranium and zirconium melt as well as the long periods of time they are maintained in a molten state. A demonstration process where uranium alloyed with 2.1 wt% Am and 1.3wt% Np showed a loss of approximately 40% of the americium mass during the casting process[5]. These losses complicate the fabrication of metal nuclear fuel and generate additional costs and overhead to the fabrication facility due to the need to clean and dispose of contamination related to vaporized transuranics, making the unmodified injection casting process unsuitable for casting fuel pins containing volatile transuranics.

Modifications have been made to the injection casting method on a bench top scale which utilizes a cover gas and a cold trap to minimize americium losses. The cover gas is maintained over the casting crucible at 0.3 atm to resist americium

vaporization, and a cold trap prevents any americium which has evaporated from leaving the casting apparatus. A small-scale demonstration was conducted which cast an alloy containing 5 wt% Am which showed americium losses on the order of 0.3% without the cover gas and a loss of 0.006% with the cover gas, indicating that this may be a viable path forward for resolving the americium volatility issue as well[6].

1.2 PROJECT OVERVIEW

The research presented here was supported by the US Department of Energy as part of a 2007 Nuclear Research Initiative (NERI) grant supporting the goals of the DOE program known as the Advanced Fuel Cycle Initiative (AFCI). The main objective of this NERI project was to develop low temperature (i.e., below ~650°C) fabrication methods for TRU-bearing U-10%Zr alloys. The work is part of a larger project in which uranium metal powder production methods and U and U-10%Zr sintering methods were also developed[4].

Powder metallurgy methods were used to fabricate U-Zr-TRU alloys using hot extrusion at relatively low temperatures (600°C) with magnesium and manganese used as surrogates for TRU elements. FIGURE (1-2) shows a plot of the vapor pressures of four elements of interest; americium, curium, magnesium and manganese versus temperature. These data shows that manganese is more prone to vaporization than curium and is similar to the americium curve. Magnesium has a far higher propensity than the rest to vaporize, making it an excellent candidate to use in a test if it can be shown that the magnesium would be completely conserved. Surrogates were necessary for this project due to americium and curium being highly radioactive elements.

Magnesium has vapor pressures higher than americium and curium, as shown in FIGURE (1-2), thus it can be expected that if the hot extrusion process results in full retention of the surrogate material it will be a good indication that americium and curium would also be retained[6]. The alpha phase uranium-zirconium alloy characteristics and hot extrusion properties of these materials are the processes which are being quantified.

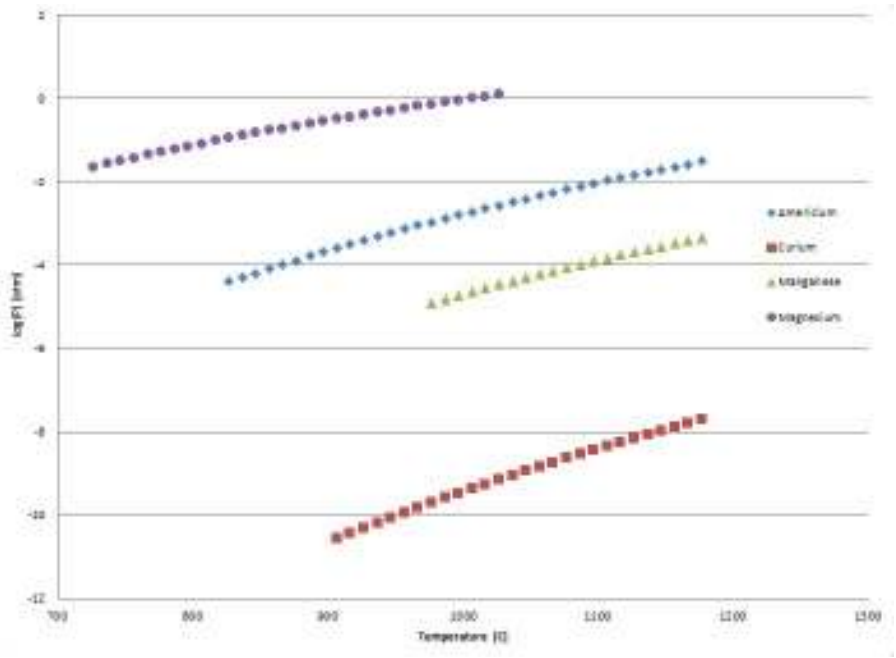

Figure (1-2) – Comparison of the vapor pressures of americium[7], curium[8], manganese[9] and mangnesium[10]. Magnesium is more prone to vaporization than both americium and curium, making it the best available surrogate.

The results of this study showed that hot extrusion is a viable means of producing TRU bearing alloys. Section 3 details the equipment and procedures utilized to produce the extrusion samples, including the adaptation of the existing uranium powder

production apparatus to produce a higher yield. Section 4 details the results of each extrusion test. There were six extrusion tests in total, with tests #3 and #5 yielding successful samples. The two extrusion samples that were produced were analyzed to show the microstructural behavior of metal powders fabricated using this method and the conservation of the surrogate materials in the process was achieved, this is detailed in Section 5. The characterization consisted of thermal analysis with a differential scanning calorimeter and image and x-ray analysis with an electron microprobe. The differential scanning calorimetry was able to identify the phase and compositional transitions the samples underwent, as well as calculating the heat capacity of the sample. The image and x-ray analysis enabled by the electron microprobe was able to identify the microstructure of the samples, as well as identify and quantify the elements that constituted the sample matrix.

It was concluded that upon fabrication of the samples the extruded product has an extremely heterogeneous structure, with almost no mixing of the constituents. When heated, these constituents mix together and form microstructures and compositions characteristic of the composition of the alloy. Also, although it was difficult to quantify precisely due to difficulty in identifying magnesium particles in the extruded sample matrix, it was concluded that magnesium was conserved in the sample with no losses observed.

2. BACKGROUND

This section describes background information relevant to the process of hot extrusion (Section 2.1), the metallurgy of the materials involved (Section 2.2) as well as the process used to convert uranium metal slugs into a fine metal powder (Section 2.3). Also, the characterization methods of x-ray spectroscopy (WDS/EDS) and differential scanning calorimetry (DSC) processes are discussed in Sections 2.4 and 2.5, respectively.

2.1 HOT EXTRUSION

Hot extrusion is a process by which a material is forced through a reduction die at a temperature above its recrystallization point. This enables the re-formation of the material from without significant work hardening, thus reducing the pressure necessary to form the desired piece. Hot extrusion is a very versatile process, capable of producing a wide variety of extruded profiles. When powder metallurgy methods are combined with hot extrusion, a high level of control is achieved over the material composition and net shape[11].

There are two methods of hot extrusion, direct extrusion and indirect extrusion. For direct extrusion, the container and die remain stationary and the ram moves to force the billet, the material to be extruded, through the die. For indirect extrusion, the billet, container and ram remain stationary as the die is forced into the billet. Illustrations of either process are shown in FIGURE (2-1).

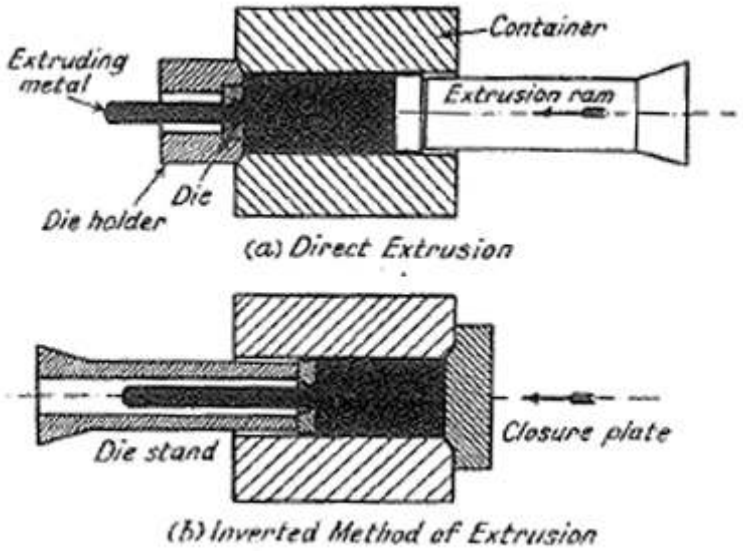

Figure (2-1) Illustrations of direct and indirect extrusion methods[11]

Direct extrusion is the easiest and least complicated from a design standpoint; however it demands higher peak force to drive the ram due to the frictional forces generated as the billet moves relative to the container and through the die. By contrast, indirect extrusion is more complex to design but it demands less driving force since the billet and container are stationary with respect to each other. A graph of the force profiles of either method is shown in FIGURE (2-2). Due to this property of either method, if extrusion of a given material is proven to be feasible using the direct extrusion method, it will likely be feasible for indirect extrusion[11].

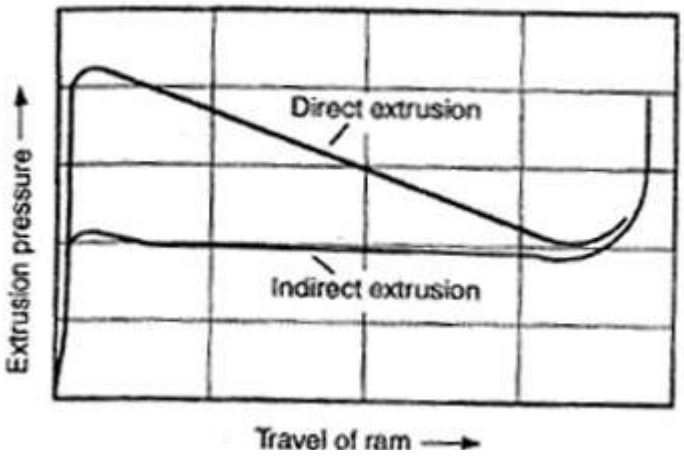

Figure (2-2) Comparison of forces encountered for direct and indirect extrusion.[12]

2.2 METALLURGICAL STUDY

The metals involved in this research are uranium, zirconium, magnesium and manganese. In addition, the extrusion canisters used to contain the powder mixtures were made of copper.

Uranium exists as three phases, α, β and γ[13]. The α phase has an orthorhombic unit cell and is stable from room temperature to 667°C. The β phase is a complex tetragonal structure with 30 atoms per unit cell and is stable in the 667°C to 772°C temperature range. The γ phase is a body-centered cubic structure and is stable from 772°C to the melting point of 1132°C. Pure metallic uranium was once considered as a candidate fuel for nuclear reactors, however it was discovered that under irradiation uranium would expand asymmetrically, which resulted in tearing and failure of the material[14]. As metal fuel technology developed, alloying additions of zirconium, molybdenum, or other metals were evaluated and U-Zr and U-Mo alloys were found to minimize tearing and reduce anisotropic swelling during irradiation[15].

Zirconium exists as two phases, α and β. The α phase has a hexagonal close packed structure and is stable up to 862°C. The β phase zirconium structure is a body-centered cubic phase and is stable from 862°C until melting at 1855°C[13].

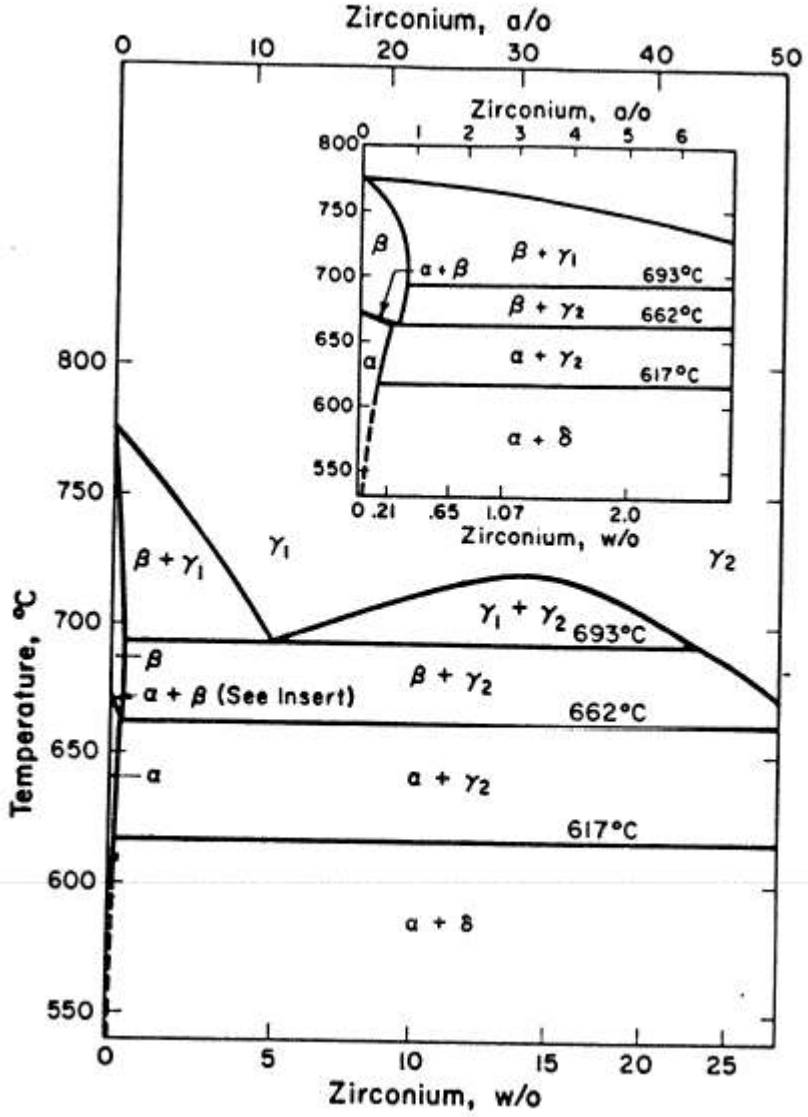

Figure (2-3) – Uranium-zirconium phase diagram, with inset.[16]

According to the binary phase diagram in Fig. 2.3, a uranium – 10 wt % zirconium alloy, which is representative of the composition utilized for fast reactor fuel pins[1], will undergo several phase transformations from room temperature to melting. At low temperatures, α uranium is stable in equilibrium with an intermetallic compound referred to as δ phase. The solubility limit of zirconium in α phase uranium is very low (less than ~0.2 wt.%), whereas to the δ phase UZr_2 intermetallic is by its very nature rich in Zr. At 617°C the δ phase material transitions into a phase referred to as γ_2, which is a body-centered cubic structure; gamma phase uranium and beta phase zirconium are mutually soluble across the entire composition under higher temperature conditions. At 662°C, the α phase transitions into the β phase, and at 693°C the β phase transitions into a γ_1 phase. At higher temperatures, the miscibility gap is not present and the alloy exists as γ-phase body-centered cubic structure until the solidus line is reached at ~ 1200°C.

Magnesium metal only exists as a hexagonal structure and it has a melting point at 650°C, as shown in FIGURE (2-4). Uranium and magnesium are non-reactive and immiscible, forming no compounds nor solid solutions[17].

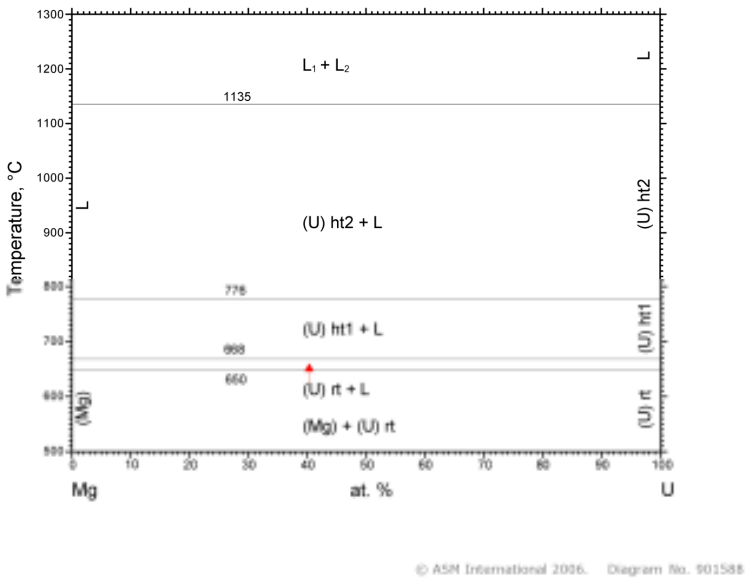

Figure (2-4) – Magnesium-uranium phase diagram. The two metals remain separate at all compositions and temperatures.[17]

In a similar fashion, magnesium also does not form any alloys with zirconium. The exception to this behavior is copper, which magnesium will interdiffuse with.

2.3 URANIUM POWDER PRODUCTION PROCESS

In order to obtain the uranium powder necessary to complete this research, a method was developed to convert solid pieces of uranium metal into powder as uranium hydride (UH_3), then that back into uranium metal[4]. When uranium metal converts to UH_3, its density decreases from 19.04 g/cm^3 to 10.9 g/cm^3, this large change in density results in the destruction of the solid chunk and a fine uranium hydride powder is produced. The uranium hydride powder produced by this method at 225°C was found to range in size from 1μm to 100μm with a volumetric mode of 44 μm[18].

The uranium hydride process is best conducted at 225°C with acid washed uranium pieces[4]. FIGURE (2-5) shows the reaction rate for hydrogen consumption by uranium versus temperature, which reaches its maximum at 225°C. The uranium pieces were acid washed using a 50-50 mixture of nitric acid and distilled water to remove surface oxidation. Surface oxidation impedes the diffusion of hydrogen into uranium, slowing or completely halting the hydride formation process. The effect may also be overcome by hydriding the uranium at a higher temperature, as temperatures above approximately 300°C increase the hydrogen diffusion rate. However at this elevated temperature, the uranium hydride powder begins to sinter, which results in larger particles and a reduced uranium powder yield[19].

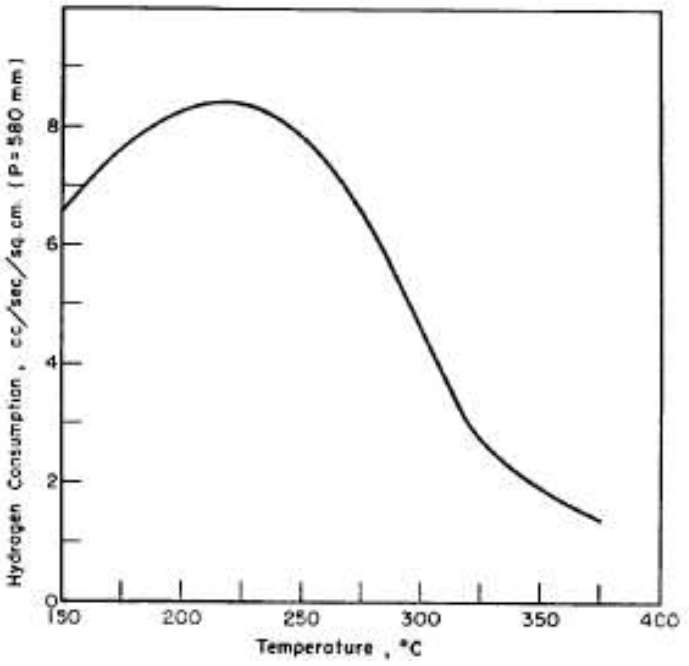

Figure (2-5) – Rate of hydrogen consumption in uranium versus temperature.[19]

After the uranium is converted to UH_3, increasing the temperature will induce thermal disassociation. This can be done at atmospheric pressure for temperatures in excess of 430°C, but uranium sintering bonds the fine particles together creating an agglomerated powder. Exposing UH_3 to a rough vacuum (less than 10 millimeters of mercury) during the dehydride procedure will induce decomposition temperatures around 300°C. As FIGURE (2-6) shows, the pressure generated by the hydrogen decomposing from the uranium hydride increases exponentially with temperature, and at 300°C exceeds the pressure of a rough vacuum, thus allowing the hydrogen gas to be evacuated from the system.

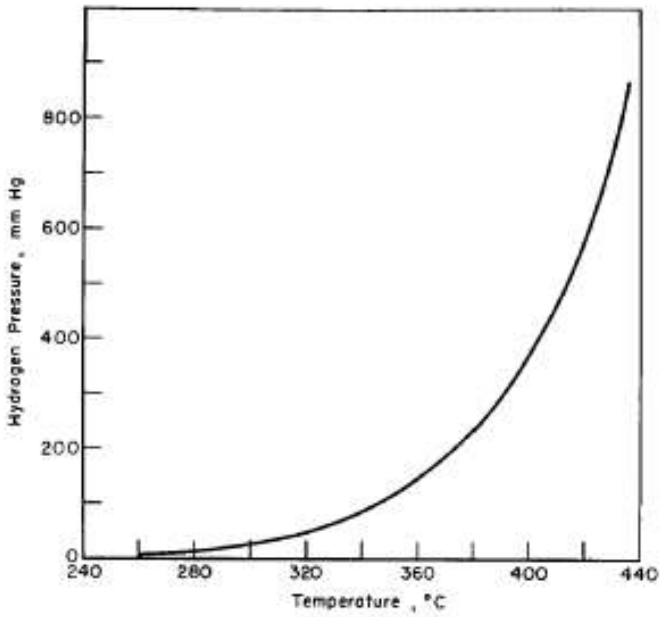

Figure (2-6) – Hydrogen pressure from uranium hydride versus temperature.[19]

2.4 WAVELENGTH AND ENERGY X-RAY SPECTROSCOPY

Wavelength dispersive x-ray spectroscopy (WDS) is a process where x-rays of a specified wavelength are diffracted by a crystal into a detector and counted. The method is typically used to detect specific characteristic x-rays generated by materials which are being investigated using an electron microprobe[20].

Characteristic x-rays are generated when an electron in a higher energy shell drops into a lower energy vacancy, a hole in an electron orbital shell. These vacancies are generated in an electron microprobe by exposing a focused electron beam onto the sample which has enough energy to overcome the threshold for ionizing an electron from an inner shell. When the electron transition occurs between orbitals of different energy levels, an x-ray is generated which possesses energy equal to the potential energy difference between the upper and lower orbital. The specific energy of these characteristic x-rays are unique for every element, and thus are reliable indicators for the presence of that element[20].

These x-rays can be detected by a variety of methods, the two most common are energy dispersive x-ray spectroscopy (EDS) and wavelength dispersive x-ray spectroscopy (WDS). EDS utilizes a detector which absorbs all of the x-rays emitted from the sample and differentiates them by energy, producing a spectrum. The energy dispersive x-ray method has the advantage of being a fast method for sample characterization, as well as resolving multiple characteristic peaks simultaneously which can quickly distinguish a majority of the elemental components of a sample. Disadvantages to EDS include the relatively large background associated with the examination of the entire x-ray spectrum arising from bremsstrahlung radiation. This

makes EDS relatively insensitive to concentrations of elements that are less than 1% in a sample and large errors are possible when used for quantitative analysis[20].

The WDS method greatly reduces the background noise and is more effective for quantitative analysis of the elemental constituents of a sample because it isolates a modal set of wavelengths for the detector to count. WDS utilizes Bragg's law to coherently scatter x-rays of a selected wavelength into a detector:

$$n\lambda = 2d \sin\theta$$

where n is an integer, λ is an x-ray wavelength, d is the lattice spacing in the diffracting crystal and θ is the incident angle of the x-ray to the plane of the crystal. FIGURE (2-7) illustrates this process.

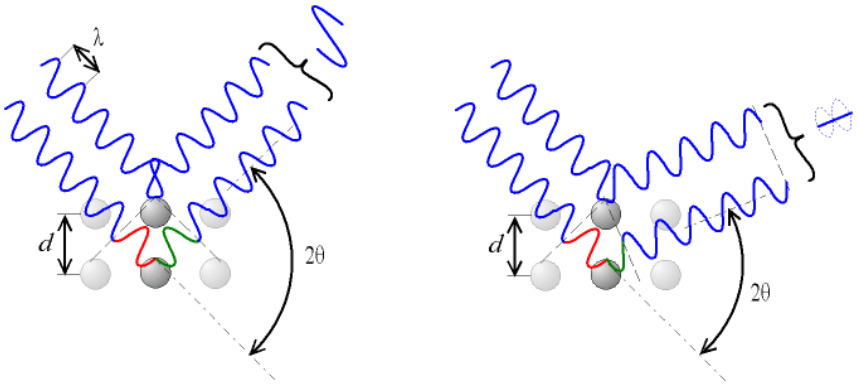

Figure (2-7) - Illustration of how Bragg's Law results in coherent scattering of wavelengths which meet the criteria (left) and mitigation of those which do not (right)[21]

By utilizing a single crystal of a known lattice spacing and adjusting the orientation of the crystal in order to obtain the desired incident angle, characteristic x-rays can be selectively diffracted into the detector[20].

2.5 DIFFERENTIAL SCANNING CALORIMETRY

Differential scanning calorimetry (DSC) is an analytical method where a sample is heated through external means and the difference between the energy absorbed or released by the sample as compared to an empty reference is recorded. This data allows for the characterization of endothermic and exothermic reactions that the sample undergoes, as a function of temperature. By measuring the heat flux required to keep the sample at the same temperature as the empty reference, the enthalpies of the reactions may be determined. Additionally, through the use of a sapphire standard in place of the normally empty reference vessel, the heat capacity of the sample can be determined from the DSC data. This data can be used to gain insight into what the microstructure of the material being analyzed is doing by observing the energy given off or taken in due to different processes occurring at characteristic temperatures. A diagram of the instrument used in this thesis is shown in FIGURE (2-8).

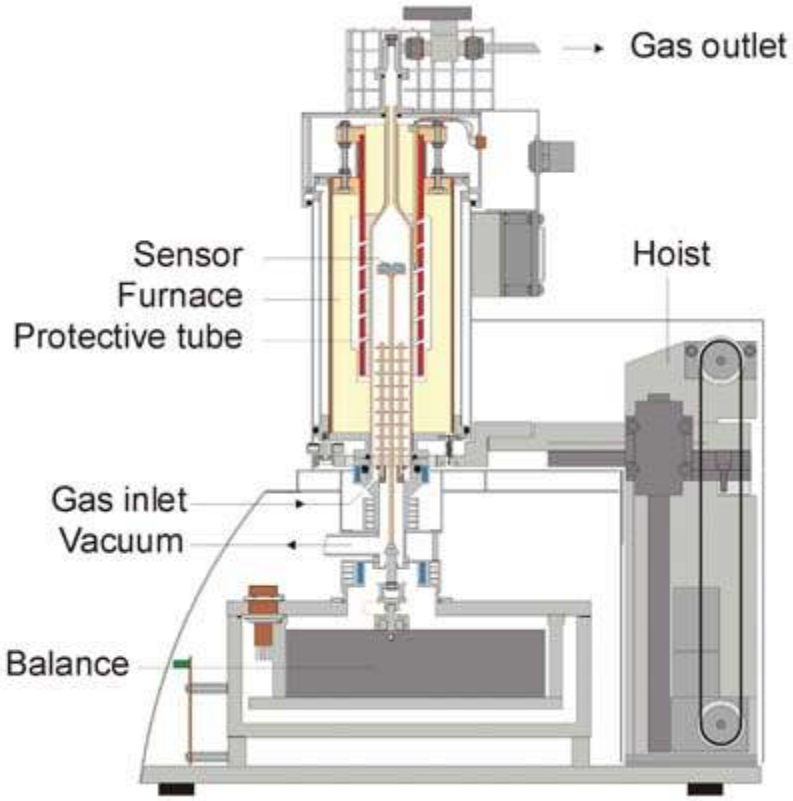

Figure (2-8) – Cross section of NETZSCH STA 409 instrument used in this work[22].

3. EXPERIMENTAL SETUP

3.1 URANIUM POWDER PRODUCTION

Uranium metal powder production was accomplished using the hydride-dehydride method mentioned in Section 2.3. The method developed by Garnetti[4] and modified by Helmreich and Sames[18] was further adapted for this project to generate larger quantities of powder. During the course of this research, three different production vessel designs were used to generate powder.

The initial setup is shown in Fig. 3-1 and is identical to the system used by Garnetti. It consisted of an atmosphere and temperature control system installed within a 2-in diameter furnace well in the floor of an inert atmosphere glovebox. The setup included an aluminum oxide crucible suspended on a steel carriage with thermal shields to insulate the system and protect the seal at the top of the furnace well. The atmosphere control equipment was a rubber stopper with an inlet and outlet copper tube; the vessel atmosphere was isolated from the glovebox and could be flowing Ar or Ar-5%H_2 or a rough vacuum. As the system was initially constructed, the mass of uranium which could be converted to powder was smaller than the mass required for an extrusion sample. This led to the establishment of the other reaction vessels described below, but a larger method was developed later for the glovebox furnace.

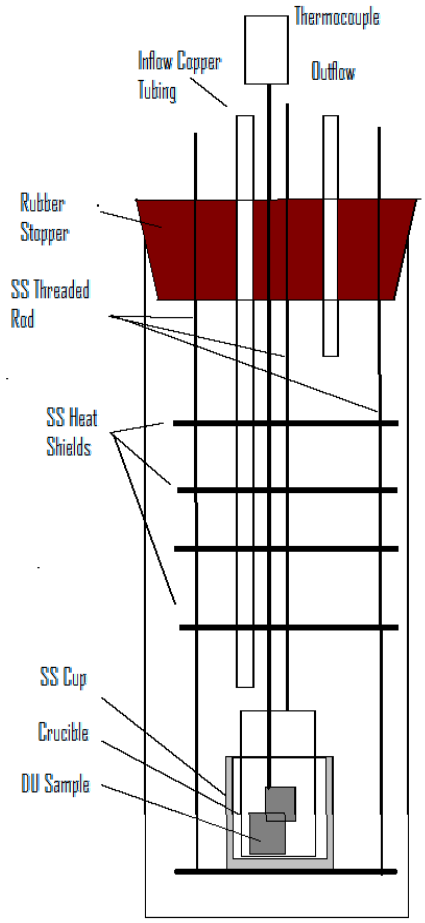

Figure (3-1) – Diagram of the hydride assembly used by D. Garnetti (not to scale) [4].

The second reaction vessel employed for this study consisted of a large steel vessel with copper sealing rings which was placed in a bench-top lab furnace. The chamber was moved into and out of the glove box for loading and unloading. This vessel was initially developed in order to study the hydriding properties of zirconium, the design requirements of which were greater than the needs for uranium hydriding. Although this vessel yielded more than enough uranium powder for extrusion samples,

the seal was unreliable, which resulted in oxidation of the uranium powder. Due to this issue, it was only used for extrusion experiments #1 and #2 before it was abandoned.

Figure (3-2) – Larger hydride-dehydride reaction system adapted from R.D. Kelley's zirconium hydride experiment.

The third reaction vessel was also a bench top apparatus, shown in FIGURE (3-3), which consisted of a large alumina tube with and alumina vessel suspended inside of it. This system produced uranium powder that had very similar properties to and in similar quantities as the glovebox apparatus. It consisted of an alumina tube assembly which internally was structured very similarly to the glovebox well system, suspended within a tubular furnace. The inlet was connected to a Ar-5%H_2 supply filtered through a moisture and oxygen scrubber system. The outlet was connected to a roughing oil vacuum.

Figure (3-3) –Larger-scale hydride-dehydride apparatus developed to produce powder for extrusion experiments.

The procedures for U metal powder production were similar for each of the systems noted above. In general, powder production proceeded in the following sequence [4]:

1. Uranium metal chunks, each approximately 2.5 cm x 2.5 cm x 0.5 cm, were first placed in nitric acid at 25% concentration for five minutes; this was performed

under argon cover gas inside of a glovebag to remove any oxide layer on the metal.

2. The acid-washed coupons were rinsed with water to remove any nitric acid prior to rinsing with ethanol and then moved into an inert atmosphere glovebox. The vacuum generated in the glovebox airlock would dry the ethanol off of the coupons.
3. The mass of the metal pieces was recorded.
4. The metal pieces were loaded into the hydride-dehydride reaction vessel and the system was prepped for processing.
5. The system was heated to 225°C and exposed to Ar-5%H_2 gas for 12 to 24 hours.
6. The process vessel was evacuated to 10^{-3} atm and heated to 300°C; for 30 minutes; hydrogen evolution was complete at this point.
7. The system was cooled down and either disassembled in the glovebox or transferred into the glovebox and disassembled to recover the metal powder. An example of the recovered material is shown in FIGURE (3-4).

The uranium powder was sieved inside the glovebox using a Dual Manufacturing Co. D-4326 sieve shaker. The sieved powder was segregated in order to remove particles larger than 90 μm in diameter. This size was selected because the Zr, Mg, and Mn powders used in the extrusion experiments were nominally ~42 μm in diameter. The mixing process was performed either manually for 30 minutes or in the bottom of the sieve shaker, typically overnight. The choice of method was typically related to when the uranium powder was available, since the packing and extrusion process required

several hours. If the powder was ready in the morning it was mixed manually for 30 minutes through shaking a jar containing the constituent powders continuously. If the powder was ready in the afternoon or evening it was shaken in a jar briefly with the other constituent powders, loaded in the base of the sieve shaker for agitation overnight, then shaken in a jar briefly once more after removal from the sieve shaker.

Figure (3-4) – Example of uranium powder product prior to classification via sieving [4]. Remains of the original uranium chunks are visible.

3.2 EXTRUSION METHOD

After the powder mixtures were prepared it was packed into the extrusion canister (still inside of the glovebox). The extrusion canisters were surplus copper canisters from previous extrusion studies [23], and the method for sealing those canisters utilized in those studies was applied here. The extrusion canister loading procedure proceeded as follows:

1. The extrusion canister was placed in a steel container for stability.
2. The canister was filled to within 3 mm (0.125 in) of the rim with loose uranium powder mixture.
3. The canister was rapidly moved from side to side in order to settle and level the powder.
4. The canister was tapped on the floor of the glovebox, also to settle and level the powder.
5. A steel ram was used in order to lightly compact and perform a final leveling of the powder within the canister.
6. Steps 2-5 were repeated until either the compacted powder was within 3 mm (0.125 in) of the rim or the uranium powder mixture was exhausted.

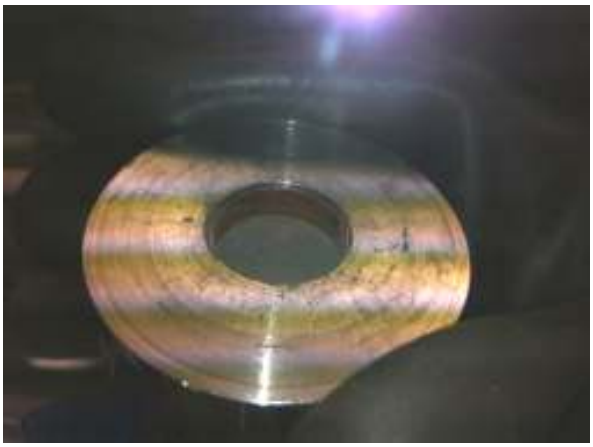

Figure (3-5) – An extrusion canister being packed with uranium powder mixture.

In multiple experiments, there would insufficient volume of the mixed uranium powder to fill the canister to the required level to form an effective seal; this extra space was filled with zirconium powder.

After the canister was filled to the appropriate level, shown in FIGURE (3-5), the lid was applied. The lid fit the inner diameter of the extrusion canister and was made of the same material. A chamfered piece of steel was placed on top of the lid and the entire loading apparatus was moved to the hydraulic press (Carver Mini-C) inside of the glovebox. The press was used to apply a compaction force of 4,500 N (0.5 t) for ~1 min, the chamfered offend of the steel ram would crimp the lid onto the extrusion canister, forming a seal.

The sealed canister was transferred from the glovebox and into a chemical fume hood designated for handling radioactive materials. In the hood, the sample was spray coated with boron nitride, shown in FIGURE (3-6). The boron nitride coating would help lubricate the canister for extrusion and would be stable at the elevated temperatures.

After the coating was dried, the canister would then be moved to the extrusion apparatus and placed in the die assemble described below. In later experiments, a copper plug was placed on top of the canister and compressed slightly to create an additional barrier against oxidation.

Figure (3-6) – The sealed sample canister after coating with boron nitride.

The extrusion apparatus consisted of four pieces of H-13 tool steel, heat treated for maxiumum strength at the extrusion temperature for each experiment. This consisted of heating the H-13 parts after machining to 1000°C for 45 minutes, then allowing the parts to cool to room temperature under forced convection, then reheating the parts to

600°C for 2 hours. The final reheating step, known as tempering the steel, was repeated for additional durability. The apparatus consisted of a ram, a container, a reduction die, and a base, shown in FIGURES (3-7) and (3-8).

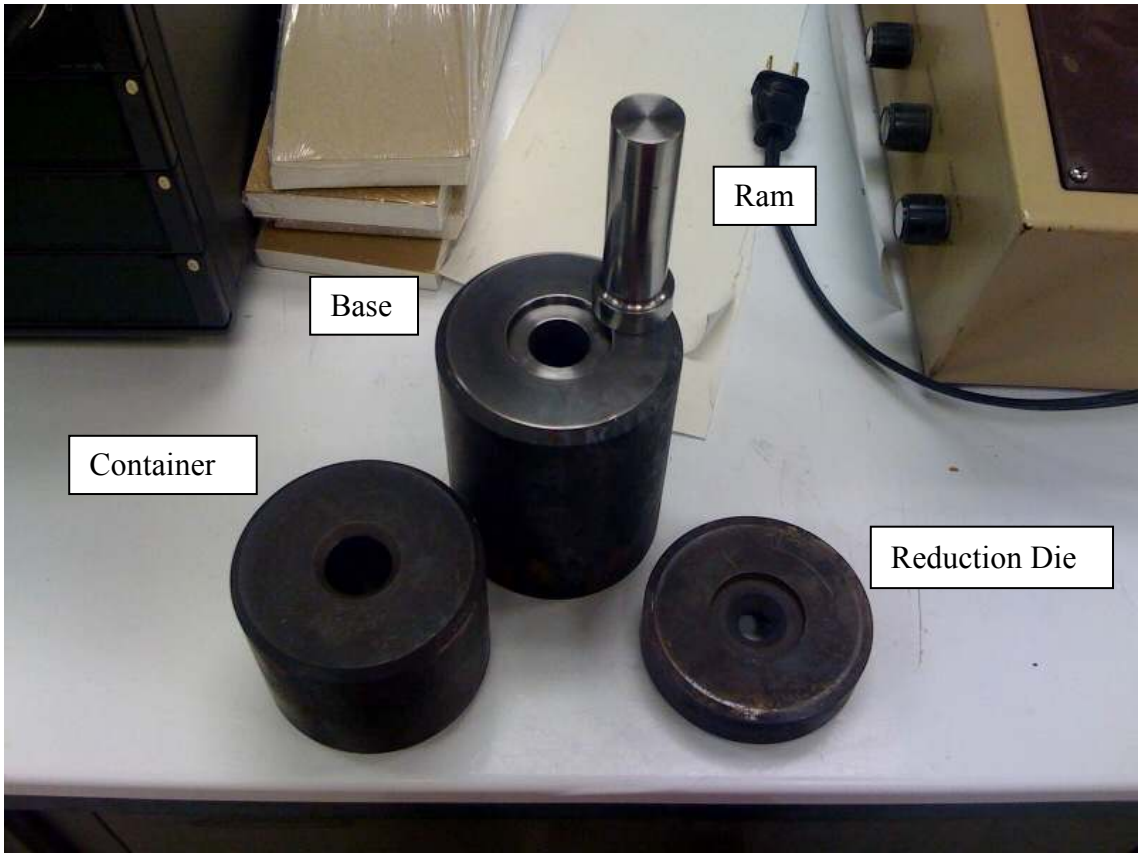

Figure (3-7) – Extrusion assembly components.

The ram was designed to snugly fit the hole in the container piece, and bear most of the stress generated transferring the force of the extrusion press into the sample. The container was designed to be slightly larger than the sample itself (0.755 in ID), to ensure against problems fitting the sample into the apparatus and would be the area where the sample would be during the heating phase of the procedure. The reduction die

was the key component in the extrusion apparatus responsible for reducing the sample to the final diameter while tolerating the most heat and stress generated in the system. Drawing from observations of previous extrusion studies [23], a reinforced version of the reduction die was chosen where after the 45° reduction cone ended a shallower relief was incorporated to add strength, while not contributing to additional stress on the sample due to friction. The smallest diameter of the reduction die was 0.25 in, resulting in a 10:1 reduction in area that the sample would be extruded through. The base served as a platform to ensure that the extrusion process fit the dimensional constraints of the extrusion press, including the available engagement of the press head. Additionally, the base was designed with a notch that could fit a thermocouple which would monitor the temperature of the reduction die near the center, enabling precise control over the temperatures that extrusions would take place.

All of these components were located within the base of a 50 ton Enerpac hydraulic press assembly. The extrusion assembly rested on top of a steel pedestal and was surrounded by a Watlow heating furnace, shown in FIGURE (3-9). The Watlow heating furnace controller interfaced with the thermocouple located within the base of the extrusion assembly for control of the extrusion temperature. The press head was cooled by a water jacket to avoid overheating the hydraulic oil in the press due to heat emitted by the Watlow furnace.

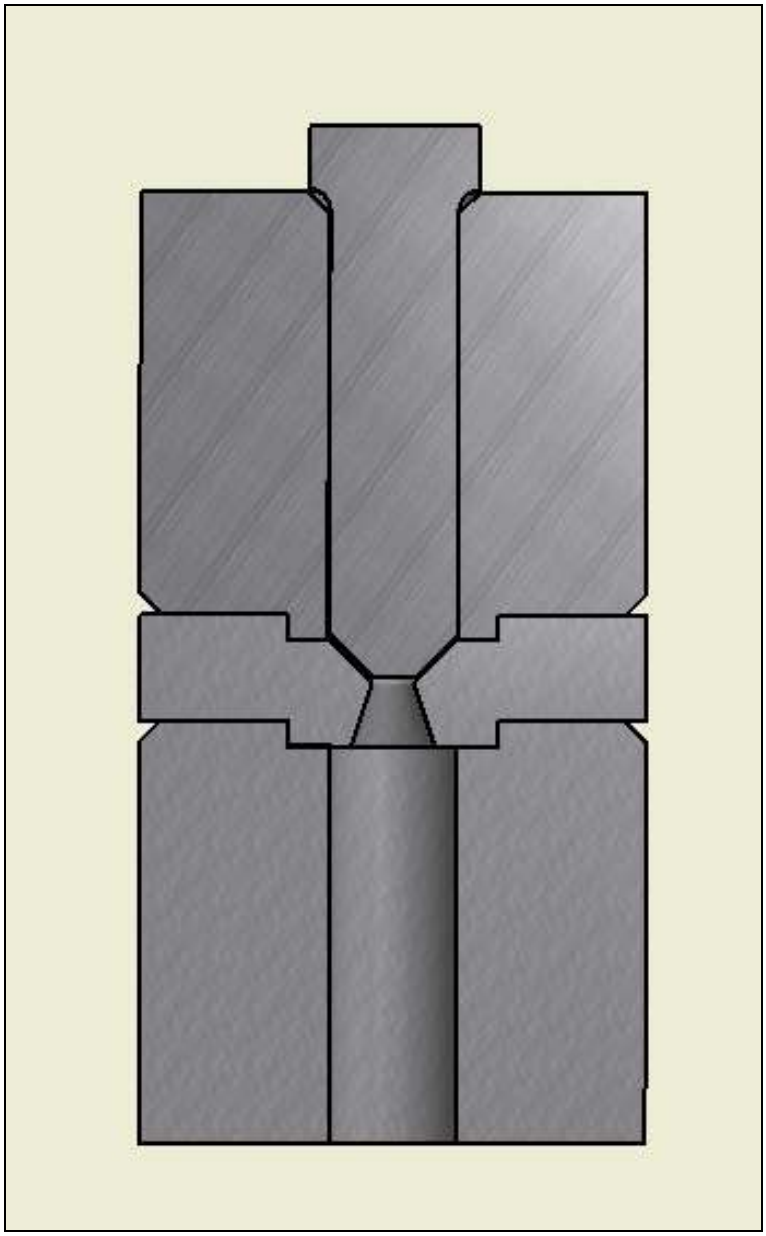

Figure (3-8) – Rendering of a cross section of the extrusion assembly.

Figure (3-9) – View of the extrusion assembly during heating. The white coating is boron nitride lubricant, to decrease resistance due to friction.

After the sample was heated in the container to the desired extrusion temperature, typically 600°C, the extrusion ram was placed on top of the sample and the pedestal attached to the press was moved into the position below the press head. The press was activated to extrude the sample by moving the ram to the full engagement designed into the extrusion apparatus. After the extrusion was complete, the press was reversed and

reset to its original position, and the pedestal would be moved out from underneath the press head to avoid overheating. The assembly was allowed to cool to ambient temperatures before extraction of the extruded sample.

4. RESULTS

Table 4.1 provides an overview of the extrusions experiments described here. The information includes the sample name, composition, process variables and notable observations from each test. The following sections describe each experiment in more detail.

TABLE (4-1) – List of experiments performed.

Extrusion Number	**Composition**	**Successful?**
1	Uranium – 10% Zirconium	N
2	Uranium – 10% Zirconium	N
3	Uranium – 10% Zirconium	Y
4	Uranium – 10% Zirconium	N
5	Uranium – 12% Zirconium – 2.5% Magnesium	Y
6	Uranium – 12% Zirconium – 5% Manganese	N

4.1 EXTRUSION APPARATUS DEMO TEST

The extrusion apparatus and method were tested initially with surrogate materials prior to extrusions involving uranium. This was done to demonstrate the performance of

the newly-machined extrusion assembly (Fig. 3-7) and extrusion procedures prior to performing experiments involving radioactive material. Copper powder was chosen for this demonstration because it is readily available and has a similar melting temperature to uranium (1086°C for Cu vs. 1132°C for U).

The copper powder was loaded into a copper canister and sealed according to the procedure described is Section 3.2. The sealed canister was loaded into the extrusion apparatus, heated to 600°C, and extruded to form a copper rod. The sample extruded with minimal resistance due to the soft and ductile nature of copper. The extruded pin had a slight curvature.

4.2 EXTRUSION 1 – U-10%Zr

The uranium powder for this experiment was generated using the second system described in Section 3.1 (Fig. 3-2). A 25 g uranium metal chunk was exposed to Ar-5%H_2 gas at 225°C for 44 hours. The powder was then dehydrided under vacuum at 325°C for 20 minutes. This procedure produced 24.3 g of uranium powder (97% conversion). 2.7 g of zirconium powder was added to the uranium powder and mixed manually in a sealed jar by shaking for 20 minutes.

The powder was then packed into a copper canister but the 27 g of uranium-zirconium powder did not completely fill the canister. Therefore, ~4 g of pure zirconium powder was added on top of the mixed powders filled the canister to enable effective extrusion. The canister was sealed with a force of 4,500 N (0.5 ton) applied to the rim of the canister lid.

The loaded canister was loaded into the extrusion apparatus and the loaded assembly was heated to 600°C. Upon reaching 600°C and allowing five minutes for the temperature to equilibrate, the extrusion ram was inserted, the heated assembly was moved into the press, and force was applied to extrude the sample. As the system pressure increased, indicated by the auditory feedback from the press pump, the press began to leak oil so the extrusion was aborted. (After the experiment, the leak was repaired and the setup procedures were adjusted to eliminate this problem.

The test sample had not reached the point where extrusion had begun before the test was aborted. Even so, the material had been deformed and reduced in volume through the compression action of the extrusion ram. The bottom of the canister formed into a cone as it conformed to the shape of the extrusion die and the canister expanded to match the diameter of the extrusion container. The canister was removed and showed no breach in containment. The canister was weighed in order to determine if any material was lost, and it was found to have a near identical weight, confirming that all of the material was contained.

4.3 EXTRUSION 2 – U-10%Zr

The uranium powder used for this experiment was produced the first system described in Section 3.1 (Fig. 3-1), which was modified to produce an additional volume of powder per run. The uranium metal was amella at 225 C for 15 hours and dehydrided at 325 C for 30 minutes. Approximately 30 g of uranium powder were produced from 85 g of uranium metal. Although this was a less efficient method of

generating uranium powder, the glovebox method was a simpler method that allowed for quick repetition and less risk of uranium powder oxidation.

The uranium powder was mixed with 3.3 grams of zirconium powder and shaken manually for 20 minutes to ensure uniformity. The mixture was then loaded and packed into a copper canister; in this case there was sufficient material such that a layer of zirconium powder was not required to make a seal with the canister lid. The canister was sealed with a force of 4,500 N (0.5 ton) applied to the rim.

The canister was loaded into the extrusion apparatus and began heating to the target extrusion temperature of 600°C. At around 400°C, the uranium powder underwent rapid oxidation which resulted in contamination within the extrusion apparatus and the press enclosure. The test was aborted and the area was decontaminated.

There was no obvious indication at the time of what caused this particular experiment to oxidize, so an adjustment was made to the procedure to incorporate an additional barrier to prevent oxygen from reaching the powder. As a result, all future extrusions incorporated an additional copper plug placed on top of the copper canister and pressed into place with the extrusion ram to form a seal.

The copper plug was a disk of copper, the diameter of the extrusion container and 6.35 mm (0.25 in) thick. The objective of this plug would be to seal off the top of the canister from the atmosphere by placing the copper plug on top of the canister and pressing it with the ram such that it would expand to the diameter of the extrusion container, prior to heating.

4.4 EXTRUSION 3 – U-10%Zr

The uranium powder was prepared by hydriding uranium in the glovebox well. For this experiment, since there was sufficient uranium powder available, the powder was sieved in order to select for particles 90 microns and lower. This was done in order to have greater control over the particle sizes being extruded and generate a more even distribution. 27 g of uranium powder were mixed with 3 g of zirconium powder and shaken thoroughly in the trough of the sieve overnight in order to ensure uniformity.

The mixed powder was then loaded and packed into a copper extrusion canister. The powder was topped with a layer of zirconium powder in order to fill the volume of the canister prior to sealing. The canister was sealed with a force of 4,500 N (0.5 ton) applied to the rim of the canister.

The copper canister was loaded into the extrusion apparatus with the copper plug placed on top of it, followed by the ram. The extrusion press was used to apply brief pressure to the ram, enough for the copper plug to expand and form a seal inside the extrusion apparatus. The extrusion apparatus was then heated up to 600°C and allowed a few minutes to equilibrate at that temperature. The force from the press was applied and the sample was extruded. Partway through the extrusion the press briefly encountered increased resistance, indicated by the auditory feedback of the hydraulic press pump, then that pressure was relieved and the extrusion then proceeded to completion.

After the test, the assembly was taken apart to extract the sample. The material had extruded mostly successfully, however the copper plug had bored through the center of the upper part of the canister. This resulted in enough pressure to separate the fully extruded portion of the pin from the top and had extruded the copper plug itself into a

long thin rod of copper that was wound up in the collection area, shown in FIGURE (4-1). The extruded portion of the pin containing the U-Zr mix, shown in FIGURE (4-2), was not adversely affected by the hyper extrusion of the copper plug, but however the partially extruded portion of the U-Zr material was exposed to the air and oxidized.

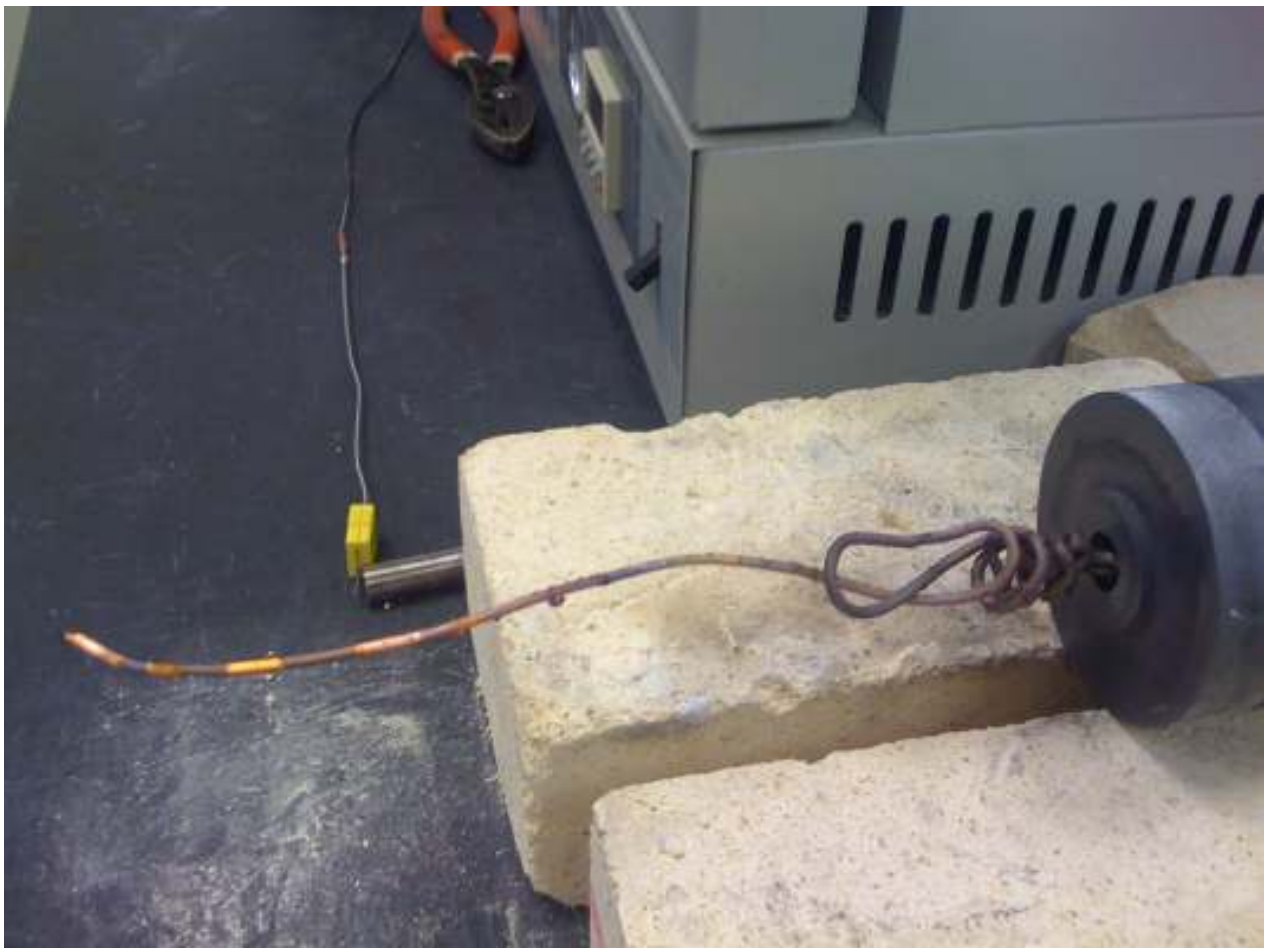

Figure (4-1) – The remains of the copper plug after the extrusion.

Figure (4-2) – The fully extruded portion of the sample measured two inches long and a quarter inch in diameter.

The sample was sectioned for analysis and further characterization. The material inside had formed a dense metal matrix, with no evidence that it had previously been powder. A 110 mg sample of the U-10%Zr alloy sample was cut from the copper liner for analysis in the differential scanning calorimeter (DSC).

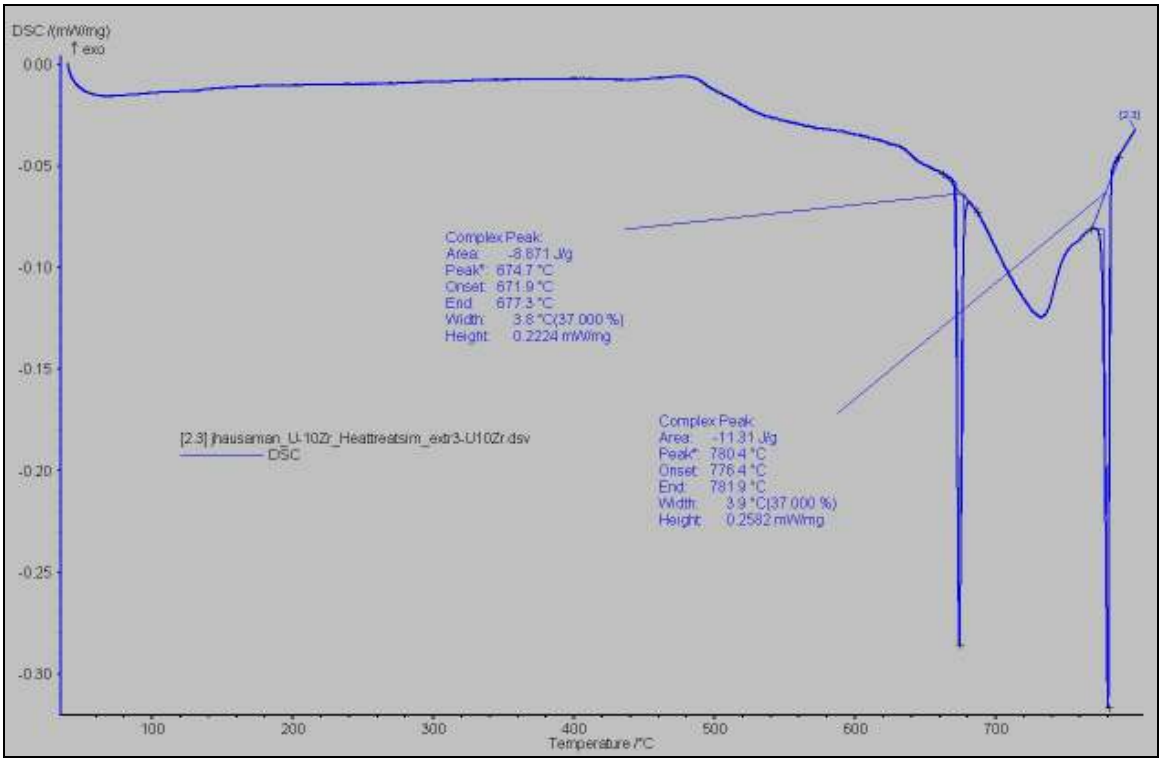

Figure (4-3) – DSC response when as fabricated sample is heated to 800°C

The alloy sample was heated at 5 K/min under flowing argon in the DSC up to 800°C. The sample was then held at 800°C for 3 hours followed by a 5 K/min reduction to room temperature. Upon heating, the DSC recorded very strong peaks at 672°C and 776°C (FIGURE 4-3), indicating either a chemical reaction or a phase change. Additionally, a very wide peak occurred starting at 500°C and peaking at approximately 730°C. The peaks were not mirrored on the cooling side of the DSC temperature program, indicating that an irreversible process had occurred.

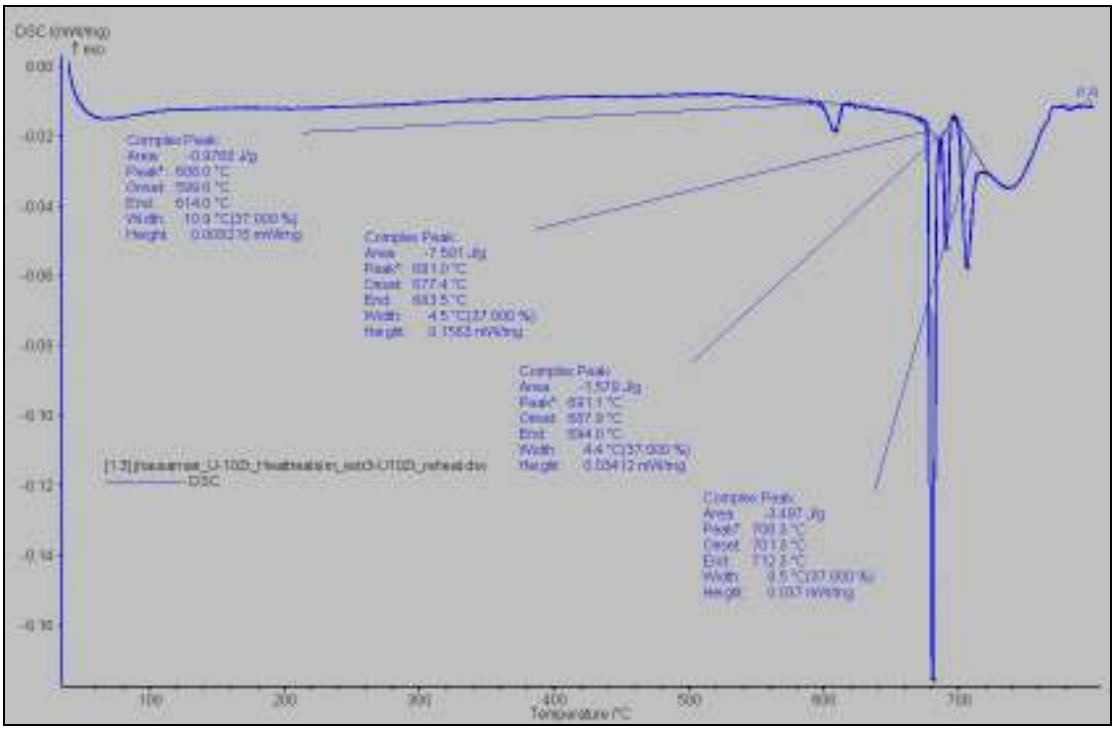

Figure (4-4) – DSC response on the second heating of the sample to 800°C

The same sample was tested through the same temperature profile in order to observe any changes which had occurred to the sample. Upon heating, many differences were observed in the sample behavior. Peaks were observed at 599°C, 677°C, 688°C and 701°C (FIGURE 4-4). Additionally, the very wide peak observed in the first measurement had diminished in magnitude although the minimum is still evident at approximately 730°C. After holding at 800°C for three hours, the observed peaks were mirrored when the sample was cooled, indicating reversible processes.

Another measurement was performed where the heat capacity of the matrix was analyzed up to 800°C. The heat capacity measurement, shown in FIGURE (4-5), showed a slight decrease as the temperature increases, this is likely due to some

oxidation occurring on the sample. Even though the sample was heated in a controlled atmosphere, the small amount of oxygen contamination present in the argon source was enough to influence the measurement. Otherwise, near 50°C the heat capacity recorded was 0.152 J/(g-K), which can be compared to a value of 0.132 J/(g-K) calculated from literature values.

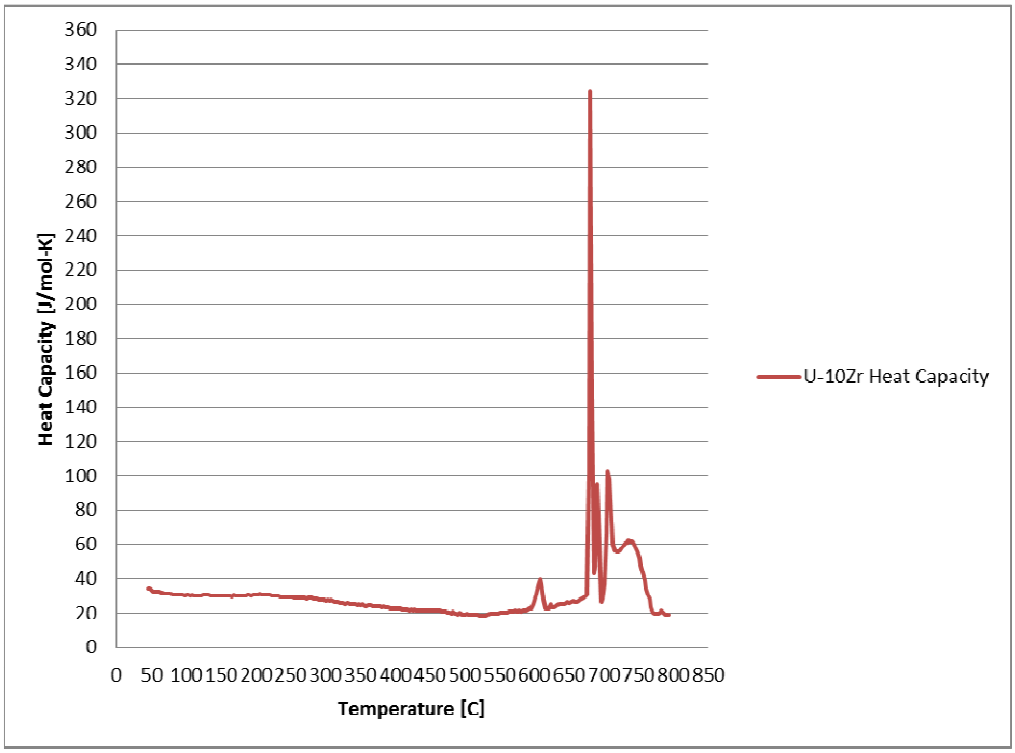

Figure (4-5) – Heat capacity of U-10%Zr

Three other sections from this alloy were prepared for microstructural characterization using an electron microprobe (Cameca SX50) and wavelength dispersive spectroscopy. One of the samples was examined in the as fabricated condition, the second sample was heat treated for one hour at 800°C, and the third

sample was heat treated at 800°C for five hours. Each sample was mounted in epoxy and polished for examination.

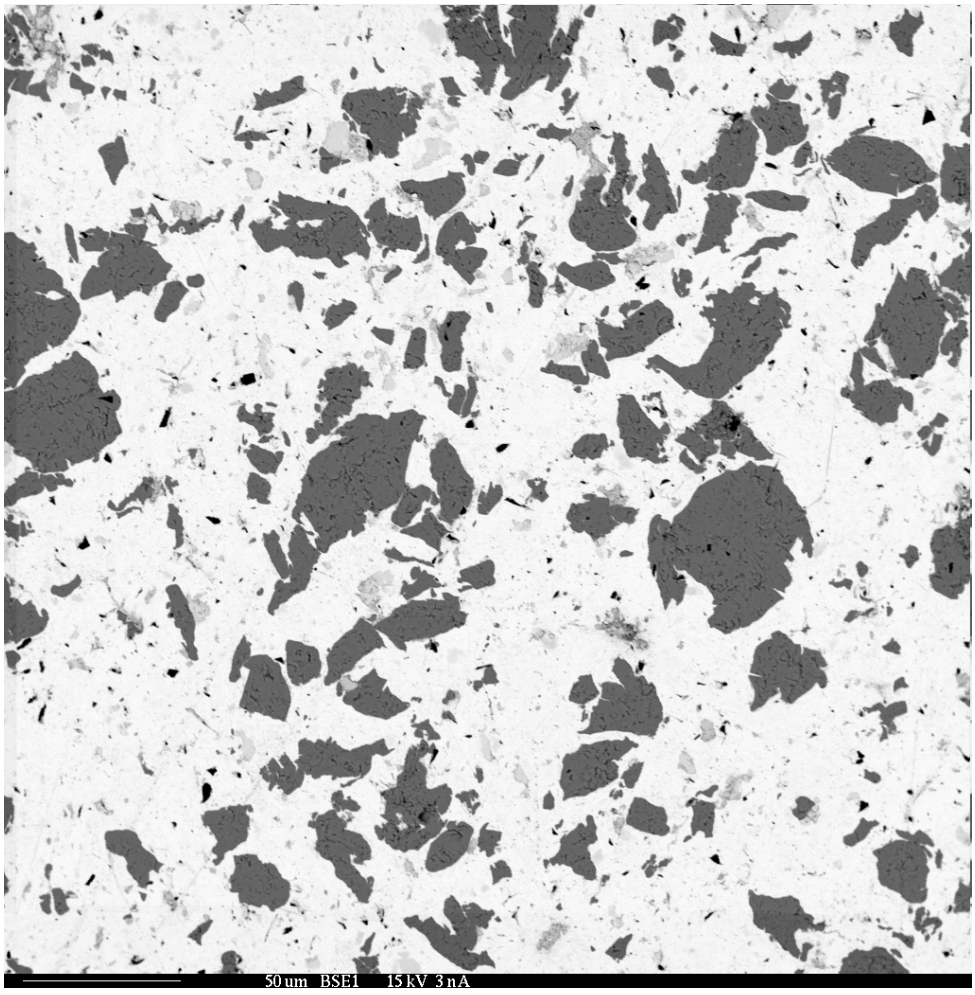

Figure (4-6) – Backscattered electron image of the as-fabricated U-10%Zr alloy from Extrusion No.3.

FIGURE 4-6 shows the matrix of sample #3 as it was fabricated after extrusion, with no heat treatments. It shows a highly heterogeneous structure with very little interdiffusion between two constituents.

Energy dispersive analysis showed that the dark grey regions were zirconium metal and the white regions were uranium metal. The light grey regions also were determined to be uranium metal. The boundaries between the distinct phases were quite sharp indicating that interdiffusion during the fabrication process was minimal. The black specks were silicon oxide that are likely polishing artifacts that had embedded itself in the matrix.

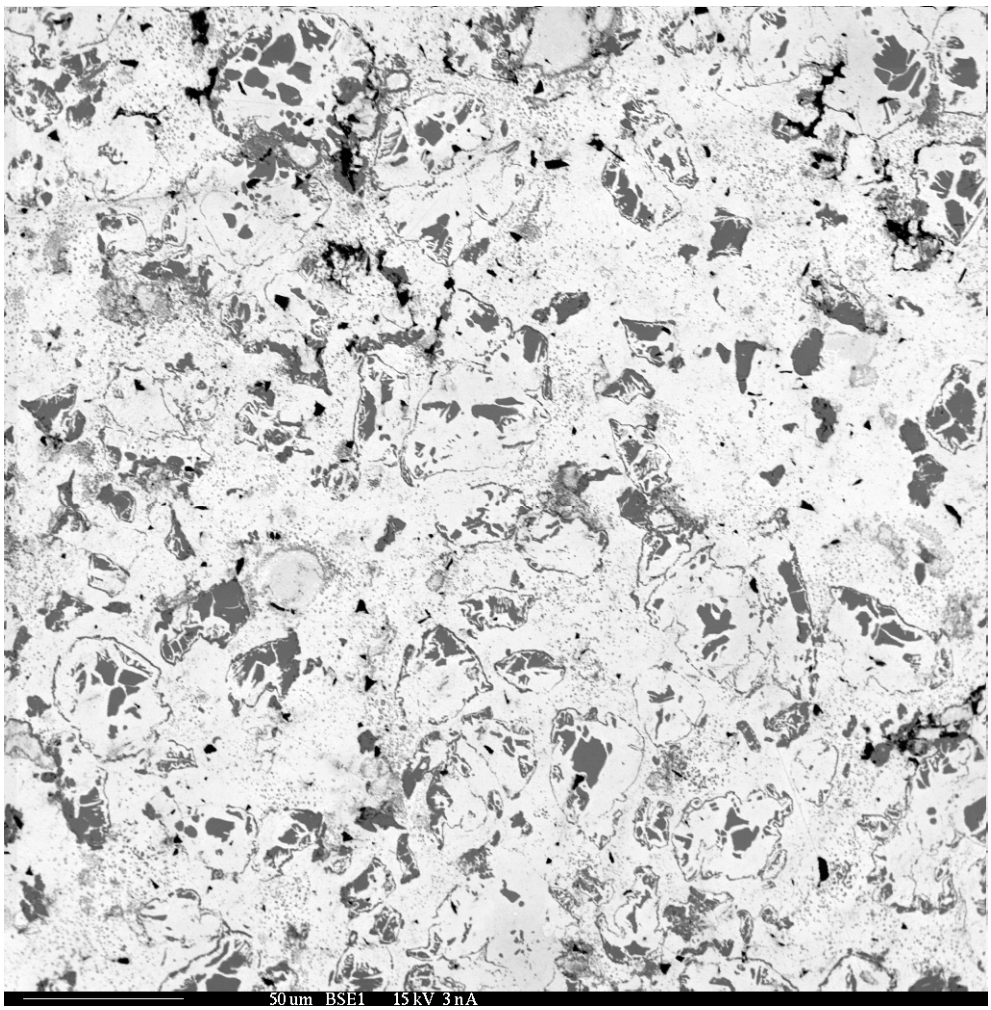

Figure (4-7) – Matrix of extrusion sample #3 after one hour of heat treatment at 800°C

After one hour of heat treatment, shown in FIGURE (4-7) the alloy microstructure was altered considerably. The zirconium and uranium elements had migrated into each other. Remnants from the original boundaries of the zirconium particles appear to be observable, possibly due to a thin layer of oxidation on the powder surfaces. The uranium appeared to be in the process of diffusing into the zirconium phases. The zirconium appeared to have diffused outward into the larger uranium phase and formed many small precipitates.

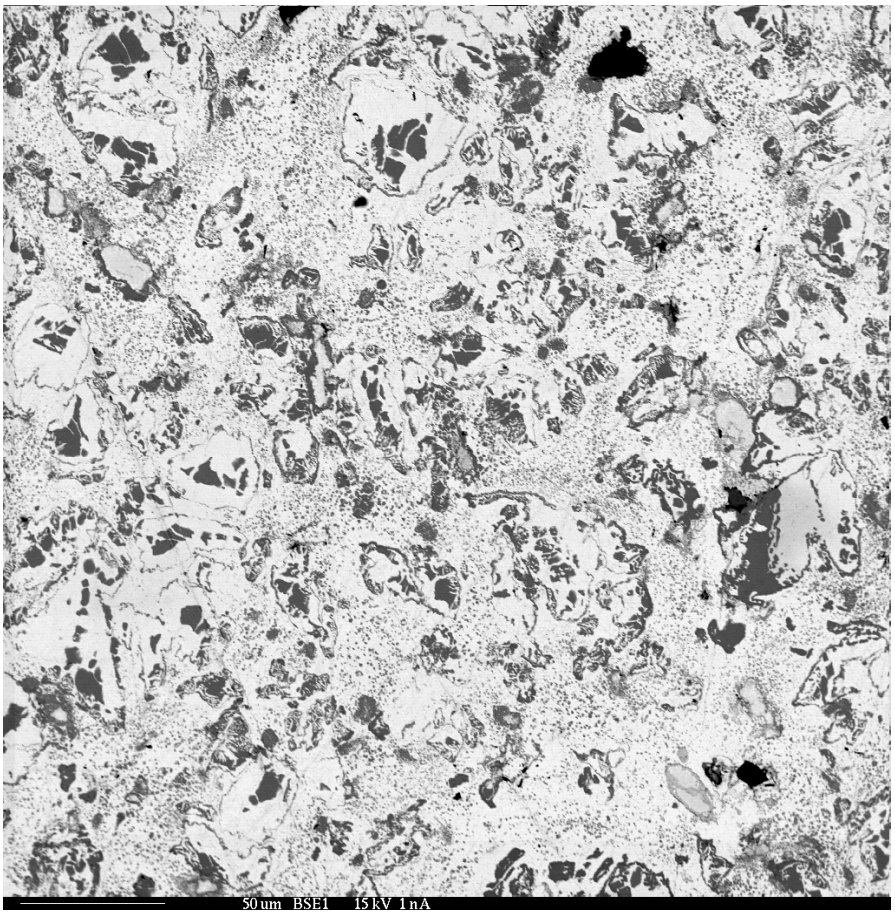

Figure (4-8) – Backscatter electron image of the matrix of sample #3 after five hours of heat treatment at 800°C

After five hours the matrix continued to undergo diffusion, shown in FIGURE (4-8). The concentration of the zirconium precipitates in the uranium phase increased, and the penetration of the uranium phase into the zirconium particles had also increased. In some particles, a lamellar structure of uranium and zirconium was observed, shown in FIGURE (4-9). This lamellar structure may be related to the intermetallic δ phase, Uzr_2.

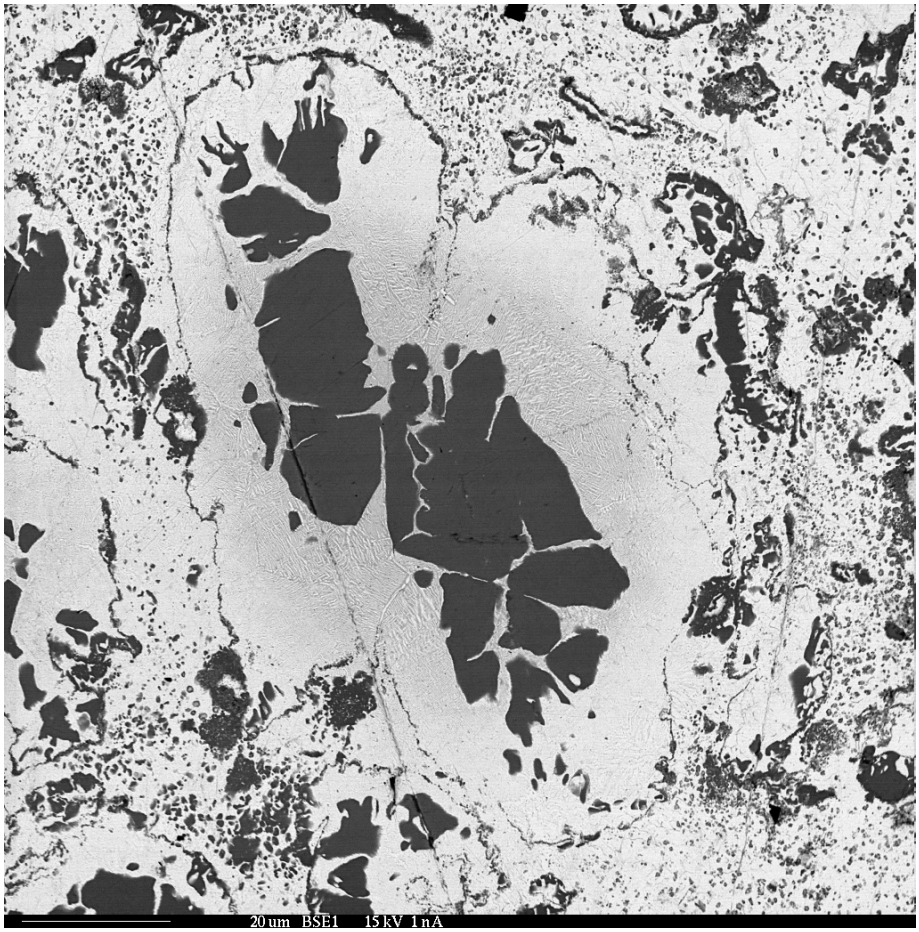

Figure (4-9) – Close up of zirconium particle after five hours of heat treatment at 800 C. The grey region within the particle is a lamellar structure consisting of uranium and zirconium metal.

4.5 EXTRUSION 4 – U-10%Zr

Following the success of the previous extrusion, the next extrusion was designed as an attempt to duplicate the sample in order to establish a reliable procedure for performing experiments. The uranium powder for this experiment was generated by hydriding and dehydriding uranium metal in the glovebox well. The uranium powder was prepared by hydriding a mix of fresh uranium metal pieces with partially amella uranium left over from the previous experiment. The material was amella at 225°C for 24 hours and dehydrided at 325°C for 30 minutes. The resulting metal powder was sieved to select for powder sizes 90 um and lower.

The 27 g of the sized uranium powder was mixed with 3 g of zirconium powder and vibrated in the base of the sieve shaker overnight in order to achieve uniformity. The mixed powder was packed into a copper canister, topped with zirconium powder, and sealed with a force of 4,500 N (0.5 ton) applied to the rim of the canister.

The canister was loaded into the extrusion apparatus with the copper plug and the extrusion ram placed on top. Force was applied from the hydraulic press at room temperature in order to deform the copper plug and form an additional seal. The extrusion apparatus was heated to 600°C and allowed to equilibrate before the extrusion. Force from the hydraulic press was applied and the sample began to extrude. Midway through the extrusion process the ram appeared to slow down and the hydraulic pump indicated that it was encountering increased resistance through auditory feedback. The pressure was suddenly relieved as a sudden movement of the extrusion ram occurred accompanied by a loud, audible crack. The extrusion was aborted and the apparatus was allowed to cool down for a follow-up inspection.

The canister had suffered a breach after it had extruded roughly a quarter of an inch though the die. As a result, the material inside was completely oxidized. It is not clear why the pressure was increasing during the extrusion operation but the extrusion ram could not be extracted from the top of the apparatus indicating that significant galling and fusion may have occurred.

4.6 EXTRUSION 5 – U-12Zr-2.5Mg

The uranium powder for this extrusion was generated in the glovebox well through hydriding and dehydriding fresh uranium metal pieces along with some partially amella material. The uranium metal was amella at 225°C for 36 hours and dehydrided at 325°C for 30 minutes. The resulting material after the dehydride procedure was selectively sieved in order to obtain uranium powder less than 90 um in diameter.

For this extrusion, it was desired to simulate a sample that would be 10% zirconium and 20% transuranic by weight. Due to the large difference in the density of the magnesium surrogate metal and transuranic elements, it was decided that the atomic percentage ratios would be used in order to obtain a representative mix of powders. The mixture consisted of 25.5 g of uranium metal powder, 3.65 g of zirconium metal powder and 0.74 g of magnesium powder. This resulted in a mixture that was 12% zirconium and 2.5% magnesium by weight. The material was then mixed thoroughly by shaking it in the base of the sieve shaker overnight.

The copper extrusion canister was packed with the mixed powder material. It was found that due to the extra volume provided by the addition of the magnesium

powder, there was no need to add a layer of zirconium to fill the canister. The canister was sealed with a force of 4,500 N (0.5 ton) applied to the edge of the rim.

The canister was loaded into the extrusion apparatus with the copper plug and the extrusion ram placed on top. Force was applied from the hydraulic press in order to deform the plug and form an additional seal. As before, the extrusion apparatus was heated to 600°C and allowed to equilibrate for a few minutes. Force was applied from the hydraulic press and the sample was extruded. Towards the end of the extrusion there was some buildup of pressure, indicated by the auditory feedback from the hydraulic pump, and some cracking sounds, however the extrusion proceeded to completion. The apparatus was allowed to cool down to room temperature before inspection and extraction of the extrusion sample.

The results were similar to the results of extrusion experiment #3. The sample had extruded a length of approximately one inch past the maximum reduction of the die before the copper plug had deformed to a point where the pressure forced it through the remainder of the canister, breaching it and severing the fully extruded section from the top of the canister. During the extrusion, the reduction die had failed and plastically deformed into a concave shape. The final dimensions of the extrusion sample, however, were not changed very much, maintaining a 3.65 mm (0.25 in) diameter. The surface of the extruded sample appeared to be textured and not smooth, shown in FIGURE (4-10), this was different as compared to sample 3.

Figure (4-10) – Photo of the extruded sample from experiment 5.

The sample was sectioned to obtain a cross section from the center of sample for characterization. The cross section showed areas of dense solid matrix interspersed with cracks and voids which originated at the copper liner of the sample and extended to three quarters the radius of the sample on average. The sample was then cut axially, and it was revealed that the cracks were in a consistent conical pattern throughout the sample, indicating that they were likely induced by stresses during the extrusion.

The cross section form the sample was mounted in epoxy and polished. Images were obtained of the matrix in the vicinity of the dense material between the stress cracks noted above.

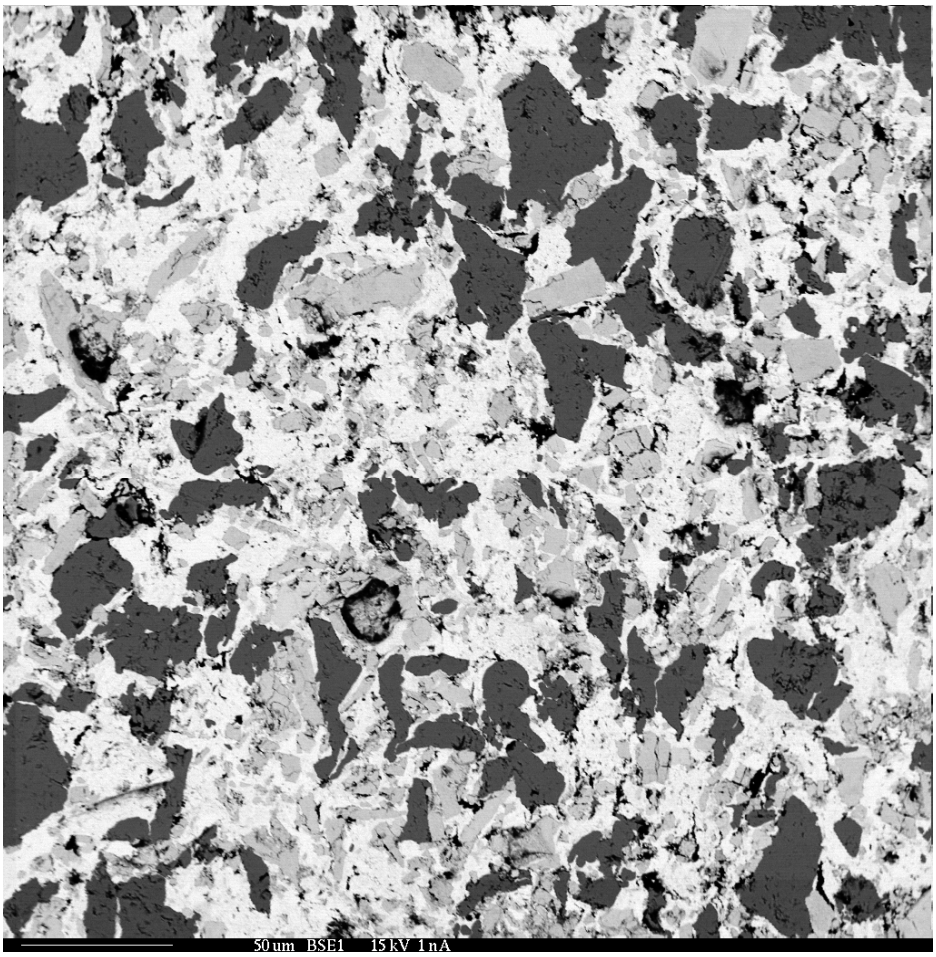

Figure (4-11) – Backscatter electron image of the matrix of extrusion sample #5

FIGURE (4-11) shows the alloy phases from the sample consisted of many variations that had not been encountered in sample #3. The material appeared to be pitted, with voids mainly concentrated in the vicinity of a medium grey phase. EDS analysis showed that the darkest grey phase was pure zirconium, the white phase was pure uranium and the medium grey phase gave a very strong uranium response, however it also contained magnesium content. An x-ray map was also taken of the sample, shown in FIGURE (4-12) which showed that some pits and voids gave a very strong

response for magnesium x-rays, while others did not. Additionally, it confirmed the EDS measurements which demonstrated that the medium grey phase consisted of a strong uranium response intermingled with a magnesium response.

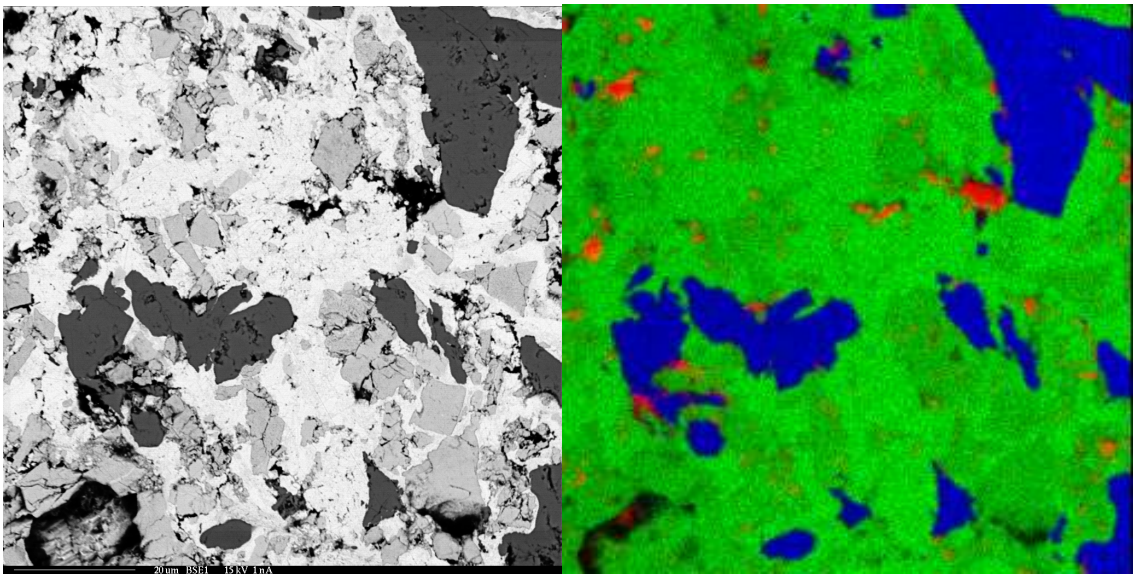

Figure (4-12) – Backscatter electron image and x-ray map of the same region in the sample. Blue indicates zirconium characteristic x-rays, green indicates uranium characteristic x-rays and red indicates magnesium characteristic x-rays.

4.7 EXTRUSION 6 – U-12Zr-5Mn

The uranium powder for this experiment was generated utilizing a bench top version of the hydride apparatus due to the glovebox well being unavailable. Pieces of fresh uranium metal were used for generating the material. The uranium was amella at 225°C for 48 hours and dehydrided at 325°C for 30 minutes. The resulting uranium powder material was sized via sieving to select for particles smaller than 90 um.

The surrogate metal chosen for this experiment was manganese, as before with the magnesium surrogate the ratio of metal powders was chosen such that the atomic percent of a sample consisting of 10% zirconium and 20% transuranic material was represented. 24.8 g of uranium powder was mixed with 3.55 g of zirconium powder and 1.6 g of manganese powder. This mixture yielded a sample which consisted of 12% zirconium and 5% manganese by weight. The mixture was shaken in the base of the sieve shaker overnight in order to ensure uniformity.

The uranium powder mixture was packed into a copper canister. Also like the magnesium sample, due to the increased volume of material available due to the addition of the manganese the canister was able to be fully packed without the need of additional material to meet the required volume to seal the canister. The canister lid was sealed with a force of 4500 N (0.5 ton) applied to the rim.

The canister was loaded into the extrusion apparatus with the copper plug and the extrusion ram placed on top. Force was applied to the extrusion ram by the hydraulic press in order to deform the copper plug and form an additional seal. The extrusion apparatus then began heating to the extrusion temperature, 600°C. At around 400°C there was a large buildup of pressure within the extrusion canister which resulted in the ejection of the extrusion ram, the copper plug and a majority of the uranium powder mixture. Upon ejection, the uranium powder mixture oxidized and the experiment was terminated.

5. ANALYSIS AND DISCUSSION

5.1 EXTRUSION #3 ANALYSIS

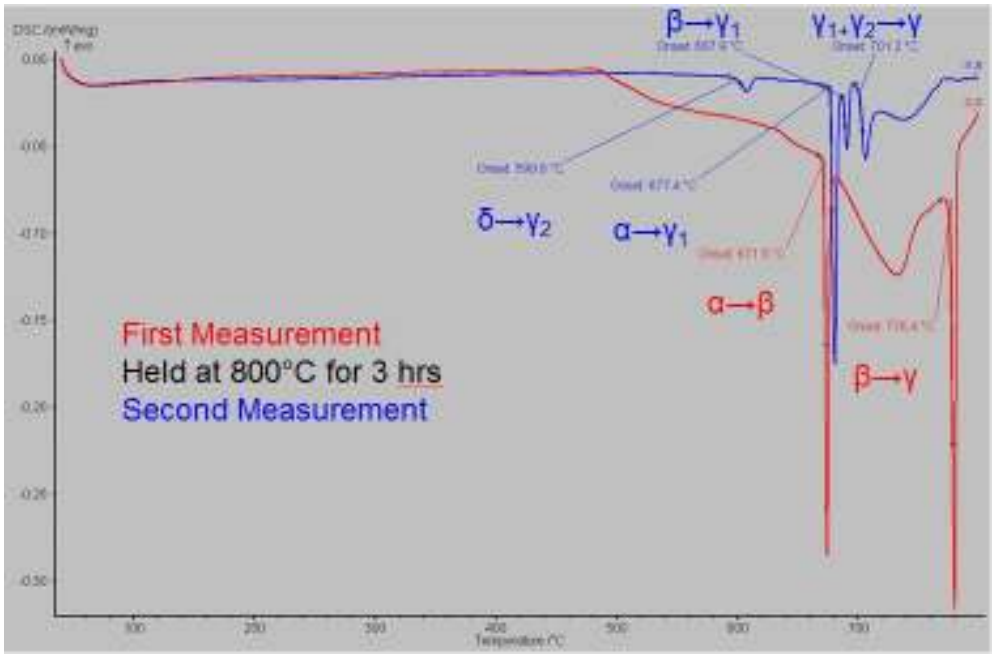

Figure (5-1) – Annotated DSC measurements of U-10%Zr alloy from extrusion #3, illustrating the phase changes that occur during heating.

FIGURE (5-1) shows a combined plot of the calorimetry curves generated during the upward temperature scan from the as fabricated U-10%Zr alloy from extrusion 3. The same 110 mg sample was examined through two DSC measurement cycles and the difference between in the initial (as fabricated) behavior and the heat treated behavior is highlighted in FIGURE (5-1). The sample was held at 800 C for 3 hours between DSC cycles.

In the first measurement, the first notable feature begins at approximately 500°C as a long endothermic drop in the signal is observed; note that this is not a distinct peak, but a broad drop in the signal indicating a possible slow process that is not a distinct reaction or phase change. This slow decrease continues for the remainder of the measurement and seems to end at approximately 730°C. In the second measurement, this feature is almost nonexistent except for a hint of a similar broad feature above the final phase change noted near 700°C. This behavior is likely characteristic of diffusion occurring in the material that results in an enthalpy of mixing. The BSE images (FIGURE 4-6) performed on the sample showed a very heterogeneous structure.

The next major features in the first measurement are two strong peaks at 672°C and 776°C. These two peaks correspond well to phase transformations that are consistent with pure uranium metal, first the transformation from the orthorhombic α phase into the tetragonal β phase, followed by the transformation into the body-centered cubic γ phase. (Note that these transition temperatures are slightly off from the literature values, but these preliminary scans were done without an extensive calibration of the instrument such that the data is only indicating the behavior without any claim on the precision or accuracy of the values.) This is consistent with the existence of a heterogeneous state in the alloy structure prior to the initial heating. No zirconium transformations are observed because they occur at temperatures greater than 800°C (phase transition at 862°C, melting at 1855°C)[13], the maximum temperature of this analysis.

After holding at 800°C for 3 hours to allow the matrix to homogenize, the sample was reheated for the second scan shown in (FIGURE 5-1). The first feature encountered

was a small peak that occurred at 599°C, followed by a series of stronger peaks at 677°C, 688°C and 701°C respectively. These measurements correspond to phase transformations that would be expected to be observed by an alloy of uranium with 10 wt% zirconium. The first transformation corresponds to the transformation of the intermetallic δ phase into a body-centered cubic γ_2 phase, followed by the orthorhombic α phase transition into the tetragonal β phase, followed by the β phase transformation into the body-centered cubic γ_1 phase. A more thorough study would be required to understand the differences between these numbers and the literature values shown on the phase diagram (FIGURE 2-3) but it is clear that the same alloy had different phase transformation characteristics after heat treatment. This implies that something has changed in the alloy, which is consistent with the observation of diffusional mixing noted in FIGURES (4-7) and (4-8).

The BSE images in FIGURES (4-6), (4-7), and (4-8) support the observations noted above. Initially, the alloy sample was extremely heterogeneous, with no mixing of the zirconium and the uranium phases. One anomaly in the uranium phase was the presence of some grains which gave a slightly lower response in the BSE image, indicative of a lower density than the surrounding material. EDS analysis confirmed that the phase was uranium, and no other metals were present, however it is possible that these small grains may be indicative of uranium hydride contamination. This explanation is somewhat confirmed by their lack of presence in either the one hour or the five hour heat treated samples.

The microstructures that evolved during heat treatment contained a lot of very interesting features (FIGURES 4-6, 4-7, 4-8). The edges of the zirconium particles prior

to heat treatment appeared to maintain an outline of the grains after diffusion had allowed for a large amount of exchange of uranium and zirconium, FIGURE (4-9) focuses on a single grain so this outline can be observed easily. This outline may be due to surface oxidation of the zirconium powder. The feature in FIGURE (4-9) is extremely thin, less than 1 μm, and does not appear hindrance the interdiffusion of the uranium and the zirconium. Zirconium that diffuses into the uranium phase appears to precipitate into extremely small grains, some less than ~1 μm wide. It is possible that these precipitates are the intermetallic Uzr_2 (δ phase) but this was not confirmable because the particles were too small for WDS quantitative analysis.

TABLE (5-1) WDS Analysis of lamellar structure

WDS Analysis	U (wt%)	Zr (wt%)	Total (wt%)	U (at%)	Zr (at%)
Lamellar_1	77.04	23.63	100.68	55.50	44.42
Lamellar_2	72.41	27.72	100.14	50.01	49.95
Lamellar_3	72.87	28.92	101.79	49.12	50.86

Uranium does not appear to have penetrated fully into to the remnant zirconium phase (FIGURE 4-9), even after five hours of heat treatment. This is consistent with by the DSC discussion above indicating some small amount of mixing taking place after three hours of heat treatment. The uranium appears to penetrate the former Zr particle in a uniform manner, indicating a uniform rate of reaction. Surrounding the zirconium core is a lamellar structure formed by both the uranium and the zirconium. This structure may be a 2-phase combination of α uranium plus the δ phase but the features are too fine

to confirm this. Analyses performed by WDS on this structure, shown in TABLE (5-1) revealed that a composition of 50 atom % uranium and 50 atom % zirconium; this corresponds to a local concentration of U-27.7 wt% Zr.

In order to establish a baseline for the accuracy of image analysis in determining the composition of the matrix, ten optical microscopy images taken of the matrix as fabricated were analyzed in ImageJ. The analysis was performed by utilizing the threshold tool to isolate and measure the areas of the different phases based on their shading. The image area analysis, shown in TABLE (5-2), resulted in a measurement of 9.5±1.2% zirconium by weight. This matches well with the measured matrix composition of 10% based on the weight of the powders measured during the canister loading procedure.

TABLE (5-2) – Image analysis results of extrusion #3.

Image	**Area % U**	**Area % Zr**	**Weight % U**	**Weight % Zr**
1	76.7	23.3	90.6	9.4
2	78.2	21.8	91.3	8.7
3	80	20	92.1	7.9
4	76.3	23.7	90.4	9.6
5	75.1	24.9	89.8	10.2
6	73.3	26.7	88.9	11.1
7	72.3	27.7	88.4	11.6
8	76.4	23.6	90.5	9.5
9	77.9	22.1	91.2	8.8
10	79.6	20.4	91.9	8.1
Average	**76.6**	**23.4**	**90.5**	**9.5**
Std Dev	2.51	2.51	1.21	1.21

5.2 EXTRUSION #5 ANALYSIS

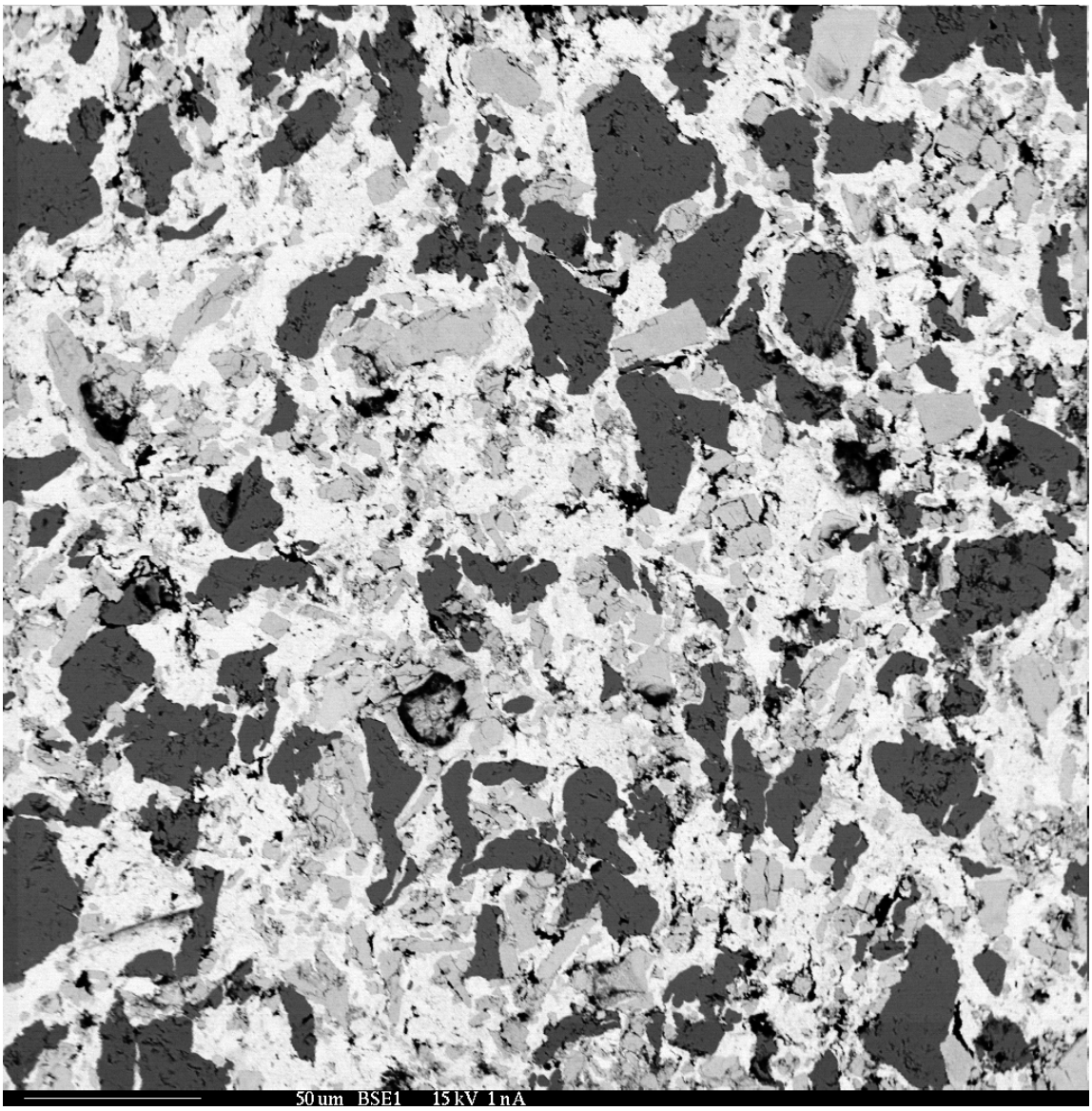

Figure (5-2) – Backscattered electron image of extrusion sample #5

FIGURE 5-2 shows an image from a polished cross section of the U-12%Zr-2.5%Mg alloy fabricated during extrusion #5. The matrix appeared to be highly

segregated, similar to the as-extruded U-10%Zr structure in FIGURE 4-6, except that there are three distinct types of solid features observable in this image. On first glance, this is consistent with the fact that uranium, zirconium, and magnesium powders were added to the extrusion canister. However, there are a few curiosities that require discussion before this obvious possibility may be confirmed.

Based on the BSE image, it would appear that there are distinct dark grey and light grey phases bonded together by a single very light phase. EDS analysis confirmed that the dark grey phase was pure zirconium and the very light phase was pure uranium, however the mid-level grey phases were found to give a strong uranium response intermingled with a weaker magnesium response, shown in TABLE (5-3). On first considerations, this was an unexpected result for the following reasons: 1) since Mg has a very low atomic number and thus large Mg particles should appear to have a very dark contrast in the presence of Zr and U, 2) the binary U-Mg phase diagram (FIGURE 2-4) indicates that these two metals are completely immiscible, and 3) the mid-level grey phases do not appear to be distorted or give any indication of mixing.

One possible explanation is that these particles are indeed the Mg particles but some BSE electrons are emanating from the U matrix below the particles in the image. It is quite possible that the microprobe beam penetrates through the magnesium particles and interacts with the uranium below it, resulting in uranium characteristic x-rays being registered by the detector. This is because electrons have a very large depth of penetration in magnesium due its low density, approximately 4 μm, as compared to uranium, which is approximately 0.1 μm[20].

TABLE (5-3) WDS analysis of extrusion #5 light grey regions

WDS Analysis	U (wt%)	Zr (wt%)	Mg (wt%)	Total (wt%)	U (at%)	Zr (at%)	Mg (at%)
Light Grey_1	92.14	0.00	1.41	93.55	87.00	0.00	13.00
Light Grey_2	99.44	0.00	0.12	99.56	98.83	0.00	1.17
Light Grey_3	100.40	0.01	0.05	100.46	99.54	0.03	0.43
Light Grey_4	87.96	0.00	2.86	90.82	75.88	0.00	24.12
Light Grey_5	14.66	3.10	32.69	50.45	4.28	2.36	93.36
Light Grey_6	93.65	0.01	0.17	93.83	98.23	0.02	1.75
Light Grey_7	93.68	0.00	0.17	93.85	98.24	0.00	1.76
Light Grey_8	91.57	0.03	1.96	93.56	82.59	0.07	17.34
Light Grey_9	88.03	0.03	0.13	88.19	98.50	0.09	1.42

Another interesting observation was the presence very large magnesium response found in the cracks found in the vicinity of the light grey particles (FIGURE 4-12). These areas had no uranium response but instead had only a strong magnesium response or no response. It is possible that the geometry introduced by the cavities may have an effect where some areas are shadowed form the x-ray sensor and others are magnified. It is also possible that during the extrusion some magnesium may have preferentially moved towards the voids.

Image analysis was performed on nine BSE images in order to quantify the composition of the matrix, shown in TABLE (5-4). The images were analyzed in ImageJ in a similar manner to the method used to analyze extrusion #3. The void areas accounted for 2.45±0.69 % of the matrix, indicating that this was a very dense structure.

Zirconium content was measured to be 20.3±1.1 % by weight and the magnesium content was measured to be 6.9±0.7 % by weight, based upon the assumption that the grey particles were 100% magnesium. Both of these values were higher than the expected values based upon the measurements taken while the powders were being packed, 12% zirconium and 2.5% magnesium by weight. Ultimately, however, this is a good indication that the magnesium particles were preserved in the matrix during the extrusion.

TABLE (5-4) – Image analysis results for extrusion #5.

Image	**Weight % U**	**Weight % Mg**	**Weight % Zr**	**Area % Void**
1	72.6	7.3	19.3	4.0
2	74.2	7.0	18.5	1.8
3	73.5	5.6	20.6	1.9
4	72.8	7.0	19.7	2.6
5	73.6	6.0	20.0	2.1
6	69.1	8.0	22.4	2.3
7	71.9	6.9	20.8	1.9
8	71.9	7.0	20.5	2.9
9	71.9	7.1	20.5	2.5
Average	**72.4**	**6.9**	**20.3**	**2.5**
Std Dev	1.5	0.7	1.1	0.7

The reasons for this discrepancy between the measurement from the image analysis and the composition of the powders are not clear. It may be possible that the powders were not mixed properly prior to loading and have an uneven distribution; however this is a fairly unlikely. Another possibility is that the flow was not uniform in the extrusion die, which led to uneven distributions of material in the sample. This is also unlikely however, as the images used for the area measurement were taken from

different areas of the cross section of the sample, unless the inhomogeneity is present axially in the sample.

6. SUMMARY AND RECOMMENDATIONS

As a result of this study, it may be concluded that under the right circumstances the extrusion process can yield a very dense matrix of heterogeneous metal particles. The metallurgical morphology of the extruded pin may be modified through heat treatment into a large array of microstructures based on the time and temperatures involved.

It was also demonstrated that magnesium metal would remain in the metal matrix after the extrusion process. As magnesium metal has a much higher vapor pressure than the transuranic elements to be integrated into metal nuclear fuel, it may be concluded that hot extrusion may be a viable method for fabrication.

The potential process methodology for the production of hot extruded fuel pins was explored and partially demonstrated from uranium powder production, to sample preparation through to extrusion. More work needs to be done to fully characterize the extrusion process through quantifying the process variables more completely (i.e., stress vs. temperature during extrusion).

If this process is utilized with uranium produced form the hydride-dehydride method, additional work must be done to develop a method to ensure that the hydrogen has been fully removed prior to canister loading.. Also, alternative canister materials, such as vanadium, should be explored in order to determine if they alter the stresses the sample undergoes during extrusion.

Ultimately, testing should be performed at a pilot production scale in order to fabricate test fuel pins that are suitable for irradiation testing and analysis. The behavior

of the highly heterogeneous structure that the hot extrusion method produces should be studied further to determine how it performs in the high temperature and high radiation environment of a nuclear reactor.

REFERENCES

[1] C. Stevenson, The EBR-II Fuel Cycle Story, The American Nuclear Society, La-grange Park, IL, 1987.

[2] H.F. McFarlane, M.J. Lineberry, The IFR Fuel Cycle Demonstration, Progress in Nuclear Energy, 31 (1997) 155-173.

[3] D.E. Burkes, R.S. Fielding, D.L. Porter, D.C. Crawford, M.K. Meyer, A US Perspective on Fast Reactor Fuel Fabrication Technology and Experience Part I: Metal Fuels and Assembly Design, Journal of Nuclear Materials, 389 (2009) 458-469.

[4] D.J. Garnetti, Uranium Powder Production via Hydride Formation and Alpha Phase Sintering of Uranium and Uranium-Zirconium Alloys for Advanced Nuclear Fuel Applications, in, Texas A&M University, College Station, TX, 2009.

[5] C.L. Trybus, S.P. Henslee, J.E. Sanecki, Casting of Metallic Fuel Containing Minor Actinide Additions, Journal of Nuclear Materials, (1993) 50-55.

[6] R.S.F. D.E. Burkes, D.L. Porter, Metallic Fast Reactor Fuel Fabrication for the Global Nuclear Energy Partnership, Journal of Nuclear Materials, (2009) 158-163.

[7] S.C. Carniglia, B.B. Cunningham, The Vapor Pressure of Americium Metal, Journal of the American Chemical Society, 77 (1955) 1502-1502.

[8] P.K. Smith, W.H. Hale, M.C. Thompson, Vapor Pressure and Crystal Structure of Curium Metal, The Journal of Chemical Physics, 50 (1969) 5066-5076.

[9] P.J. Spencer, J.N. Pratt, A Study of the Vapour Pressure of Manganese Using a New High-Temperature Torsion - Effusion Apparatus, British Journal of Applied Physics, 18 (1967) 1473-1478.

[10] J.F. Smith, R.L. Smythe, Vapor Pressure Measurements Over Calcium, Magnesium and Their Alloys and the Thermodynamics of Formation of CaMg2, Acta Metallurgica, 7 (1959) 261-267.

[11] C.E. Pearson, The Extrusion of Metals, Wiley, New York, 1953.

[12] P.R. Roberts, B.L. Ferguson, Extrusions of Metals Powders, International Materials Reviews, 36 (1991) 62-79.

[13] A.N. Holden, W.E. Seymour, Intermediate Phase in the Uranium-Zirconium System, Journal of Metals, 8 (1956) 1312-1316.

[14] S.F. Pugh, Swelling in Alpha Uranium Due to Irradiation, Journal of Nuclear Materials, 4 (1961) 177-199.

[15] D. Keiser, J. Kennedy, B. Hilton, S. Hayes, The Development of Metallic Nuclear Fuels for Transmutation Applications: Materials Challenges, Journal of the Minerals, Metals and Materials Society, 60 (2008) 29-32.

[16] H.H. Chiswick, Advances in the Physical Metallurgy of Uranium and Its Alloys, Geneva Conference Papers, (1958) 713-735.

[17] C.J.B. Nayeb Hashemi A.A., Mg-U (Magnesium-Uranium), in, Binary Alloy Phase Diagrams, 2nd Ed., Ed. T.B. Massalski, 1990, pp. 2564-2565.

[18] W.J.S. G.W. Helmreich, D.J. Garnetti, S.M. McDeavitt, Uranium Powder Production Using a Hydride-Dehydride Process, in: American Nuclear Society-Summer, American Nuclear Society, San Diego, CA, 2010.

[19] H.H. Hausner, J.L. Zambrow, Powder Metallurgy of Uranium, Nuclear Science and Engineering, 1 (1955) 92-101.

[20] J. Goldstein, Scanning Electron Microscopy and X-ray Microanalysis, 3rd ed., Springer, New York, NY, 2003.

[21] C.D.N. Chan, in: L.d. bragg.png (Ed.), Wikimedia Commons, 2004, pp. Bragg's law: according to the 2θ deviation, the phase shift causes constructive (left picture) or destructive (right picture) interferences.

[22] J. Blumm, Improving Zirconia Ceramics through Thermoanalytical Characterization, in: Ceramic Industry, Selb, Germany, 2005.

[23] A. Totemeier, Evaluation of a Zirconium-Matrix Cermet for the Storage and Transmuation of Transuranic Isotopes, in, Purdue University, West Lafayette, Indiana, 2006.

VITA

Jeffrey Stephen Hausaman

B.S., Nuclear Engineering, Texas A&M University 2008

Department of Nuclear Engineering

c/o Dr. McDeavitt

Texas A&M University

College Station, TX 77843-3133